ELSEVIER

Contents lists available at ScienceDirect

Journal of Computational and Applied Mathematics

journal homepage: www.elsevier.com/locate/cam



Low regularity primal-dual weak Galerkin finite element methods for convection-diffusion equations



Chunmei Wang a,*,1, Ludmil Zikatanov b,2

- ^a Department of Mathematics & Statistics, Texas Tech University, Lubbock, TX 79409, USA
- ^b Department of Mathematics, Penn State University, University Park, PA, 16802, USA

ARTICLE INFO

Article history: Received 10 December 2019 Received in revised form 27 February 2021

MSC: primary 65N30 65N15 65N12 74N20 secondary 35B45 35J50 35J35

Keywords:
Low regularity solutions
Primal-dual finite element method
Weak Galerkin
Convection-diffusion equations

ABSTRACT

We consider finite element discretizations for convection–diffusion problems under low regularity assumptions. The derivation and analysis use the primal–dual weak Galerkin (PDWG) finite element framework. The Euler–Lagrange formulation resulting from the PDWG scheme yields a system of equations involving not only the equation for the primal variable but also its adjoint for the dual variable. We show that the proposed PDWG method is stable and convergent. We also derive a priori error estimates for the primal variable in the H^ϵ -norm for $\epsilon \in [0, \frac{1}{2})$. A series of numerical tests that validate the theory is presented as well.

© 2021 Elsevier B.V. All rights reserved.

1. Introduction

In this paper we consider the model convection-diffusion problem for an unknown function u satisfying

$$-\nabla \cdot (a\nabla u - \boldsymbol{b}u) = f, \quad \text{in} \quad \Omega,
 u = g_1, \quad \text{on} \quad \Gamma_D,
 (-a\nabla u + \boldsymbol{b}u) \cdot \boldsymbol{n} = g_2, \quad \text{on} \quad \Gamma_N.$$
(1.1)

Here, $\Omega \subset \mathbb{R}^d (d=2,3)$ is an open bounded domain whose boundary $\partial \Omega$ is a Lipschitz polyhedron (polygon for d=2) with $\Gamma_D \cup \Gamma_N = \partial \Omega$. Further, \boldsymbol{n} is the unit outward normal vector to Γ_N . Assume the Dirichlet boundary value satisfies the low regularity of $g_1 \in L^2(\Gamma_D)$ as opposed to the usual $H^{\frac{1}{2}}$ regularity. We further assume that the diffusion tensor and the convection vector \boldsymbol{b} are smooth enough, namely, $a = \{a_{ij}\}_{d \times d} \in [W^{1,\infty}(\Omega)]^{d \times d}$, $\boldsymbol{b} \in [W^{1,\infty}(\Omega)]^d$. In addition, we assume that a(x) is symmetric and positive definite; i.e., there exists a constant $\alpha > 0$, such that

$$\xi^T a \xi > \alpha \xi^T \xi, \quad \forall \xi \in \mathbb{R}^d.$$

E-mail addresses: chunmei.wang@ttu.edu (C. Wang), ludmil@psu.edu (L. Zikatanov).

- ¹ The research of Chunmei Wang was partially supported by National Science Foundation (NSF) Award DMS-1849483.
- ² The work of Zikatanov was supported in part by National Science Foundation (NSF) DMS-1720114 and DMS-1819157.

^{*} Corresponding author.

Some of the results presented below hold also for piece-wise smooth diffusion and convection coefficients and we indicate this where appropriate.

As is often observed, (see e.g. [1,2] and the references therein) the standard Galerkin finite element approximation for the convection-diffusion may exhibit nonphysical oscillations, especially in convection dominating regime when the eigenvalues of a are small compared to the size of b and prohibitively small mesh sizes are required for providing accurate approximation. A variety of numerical stabilization techniques have been developed to resolve this challenge in the past several decades such as fitted mesh methods [2,3], fitted operator methods [2], methods using approximations of the fluxes [4,5], discontinuous Galerkin methods and mixed finite element methods. Such methods usually provide upwind-type schemes and are applicable to the problems of complicated domains or layer structures. Among the various upwind schemes, the streamline upwind Petrov-Galerkin method proposed by Hughes and Brooks is an efficient numerical method [6.7] in improving the stability of the standard Galerkin method through the use of an additional stabilization term in the upwind direction. It is known, however, that upwind methods introduce a great deal of artificial diffusion which is not desirable, especially in spatial dimensions $d \ge 2$ [6,7]. Bakhvalov [8] proposed the optimization of numerical meshes, where the meshes were generated from projections of an equidistant partition of layer functions. Another effective idea of piecewise-equidistant meshes was proposed by Shishkin [9]. An efficient adaptive method has been proposed [10,11] to address a variety of difficulties including layers [12]. The discontinuous Galerkin (DG) method [13-17] is an effective technique for solving conservation laws for elliptic problems. Furthermore, DG schemes include a upwinding which is equivalent to the stabilization for the convection-diffusion problems [2,18-25]. Recently, Burman and He [26] developed a primal-dual mixed finite element method for indefinite advection-diffusion equations with optimal a priori error estimates in the energy and the L^2 norm for the primal variable when the Pecket number is low. In [27], Burman, Nechita and Oksanen devised a stabilized finite element method for a kind of inverse problems subject to the convection-diffusion equation in the diffusion-dominated regime. Some error estimates in local H^1 or L^2 norms were derived for their numerical approximations.

Our goal is to derive and analyze a finite element discretization for the convection–diffusion problem (1.1) using the primal–dual weak Galerkin (PDWG). The PDWG framework provides mechanisms to enhance the stability of a numerical scheme by combining solutions of the primal and the dual (adjoint) equation. Such technique was successfully used for the constructing approximations to the elliptic Cauchy problems [28,29], elliptic equations in non-divergence form [30], and Fokker–Planck equations [31]. A similar idea has been explored by Burman [26,27,32–38] in other finite element contexts. Our choice of using the PDWG framework is mainly motivated by the fact that the PDWG techniques are natural for deriving error estimates under low regularity assumptions. They also allow for general polyhedral (not necessarily simplicial) finite elements. Methods for convection–diffusion equations on such general meshes have been also developed in the context of Virtual Finite Element methods (VEM) [39–41], DG methods and Hybrydized DG methods (HDG) [42–46]. While in many cases variants of the HDG, VEM and WG methods are shown to be equivalent [47–49], for low regularity solutions such equivalences are of little help in deriving error estimates. Our PDWG scheme is a novel approach allowing for a priori error estimates for the primal variable in H^{ϵ} -norm for $0 \le \epsilon < \frac{1}{2}$ when the solution does not have regularity higher than H^1 .

Compared with other existing finite element methods, our analysis of error estimates is based on the $H^{2-\epsilon}(\Omega)$ ($0 \le \epsilon < \frac{1}{2}$) regularity assumption for the solution of the dual problem with homogeneous boundary data, so that the corresponding error estimate for the primal (main) variable requires merely the $H^{\tau}(\Omega)$ regularity for some $\tau < 1$ when C^0 -WG elements are employed. This low regularity assumption on u is important because the weak solution to the model problem (1.1) as characterized by (2.1) may have only H^s regularity with 0 < s < 1 when the Dirichlet data is only in $L^2(\Gamma_D)$. To our knowledge, regularity results for discontinuous boundary data are rather difficult to establish albeit the solutions can be approximated. In such cases, the solution of the continuous problem may not be in a classical Sobolev spaces. For detailed theoretical results we refer to a monograph by J. Chabrowski [50], work by M. Costabel [51], and further remark that such results are discussed by N. Wiener [52,53] as early as the beginning of the last century.

The paper is organized as follows. Section 2 is devoted to a discussion/review of the weak differential operators as well as their discretizations. In Section 3, the primal-dual weak Galerkin algorithm for the convection-diffusion problem (1.1) is proposed. Section 4 presents some technical results, including the critical *inf-sup* condition, which plays an important role in deriving the error analysis in Section 6. The error equations for the PDWG scheme are derived in Section 5. In Section 6, the error estimates in an optimal order are derived for the primal-dual WG finite element method in some discrete Sobolev norms. Finally in Section 7, a series of numerical results is reported to demonstrate the effectiveness and accuracy of the numerical method developed in the previous sections.

2. Preliminaries and notation

Throughout the paper, we follow the standard notation for Sobolev spaces and norms. For any open bounded domain $D \subset \mathbb{R}^d$ with Lipschitz continuous boundary, we use $\|\cdot\|_{s,D}$ and $|\cdot|_{s,D}$ to denote the norm and seminorm in the Sobolev space $H^s(D)$ for any $s \geq 0$, respectively. The norms in $H^s(D)$ for s < 0 are defined by duality with the norms in $H^{|s|}(D)$ [54]. The inner product in $H^s(D)$ is denoted by $(\cdot, \cdot)_{s,D}$. The space $H^0(D)$ coincides with $L^2(D)$, for which the norm and the inner product are denoted by $\|\cdot\|_D$ and $(\cdot, \cdot)_D$, respectively. When $D = \Omega$, or when the domain of integration is clear from the context, we drop the subscript D in the norm and the inner product notation. For convenience, throughout the paper, we

use "\(\times\)" to denote "less than or equal to" up to a generic constant which is independent of important parameters such as the mesh size and physical parameters.

The weak formulation of the convection–diffusion model problem (1.1) is: find $u \in L^2(\Omega)$ satisfying

$$(u, \nabla \cdot (a\nabla w) + \boldsymbol{b} \cdot \nabla w) = -(f, w) + \langle g_2, w \rangle_{\Gamma_N} + \langle g_1, a\nabla w \cdot \boldsymbol{n} \rangle_{\Gamma_D}, \quad \forall w \in W,$$

$$(2.1)$$

where $W = \{w \in H^{2-\epsilon}(\Omega): w|_{\Gamma_0} = 0, a\nabla w \cdot \boldsymbol{n}|_{\Gamma_N} = 0\}$ for some fixed $\epsilon \in [0, \frac{1}{2})$.

The dual problem corresponding to this primal formulation is: for a given $\psi \in H^{-\epsilon}(\Omega)$, find $\lambda \in W$ such that

$$(v, \nabla \cdot (a\nabla \lambda) + \mathbf{b} \cdot \nabla \lambda) = (\psi, v), \quad \forall v \in H^{\epsilon}(\Omega).$$

$$(2.2)$$

In the following we assume that the solution to the dual problem is $H^{2-\epsilon}(\Omega)$ -regular and satisfies the following regularity estimate

$$\|\lambda\|_{2-\epsilon} \le \|\psi\|_{-\epsilon}. \tag{2.3}$$

This regularity assumption also implies that when $\psi \equiv 0$, then the dual problem (2.2) has a unique solution $\lambda \equiv 0$.

Notice that the primal and the dual equation are unrelated to each other in the continuous model. However, combining the discrete primal equation with the discrete dual equation through some stabilization terms in the context of weak Galerkin finite element methods gives rise to an efficient numerical scheme.

3. Discrete weak differential operators

Denote by $\mathcal{L} := \nabla \cdot (a\nabla)$ the diffusion part of the differential operator in (1.1). The operator \mathcal{L} and the gradient operator are the two principle differential operators used in the weak formulation (2.1) for the convection–diffusion equation (1.1). This section briefly introduces a weak version of \mathcal{L} and the gradient operator; see [55] for details.

Let \mathcal{T}_h be a finite element partition of the domain Ω into polygons in 2D or polyhedra in 3D which is *shape regular* if and only if the following trace and inverse inequalities hold for any $T \in \mathcal{T}_h$, $\phi \in H^{1-\theta}(T)$ and ψ -a polynomial on $T \in \mathcal{T}_h$:

$$\|\phi\|_{\partial T}^{2} \lesssim h_{T}^{-1} \|\phi\|_{T}^{2} + h_{T}^{1-2\theta} \|\phi\|_{1-\theta}^{2}, \qquad \|\psi\|_{\partial T}^{2} \lesssim h_{T}^{-1} \|\psi\|_{T}^{2}. \tag{3.1}$$

We refer the reader to [55] for details and discussion of sufficient conditions on the partition so that these inequalities hold.

Further, we denote by \mathcal{E}_h the set of all edges or flat faces in \mathcal{T}_h and by \mathcal{E}_h^0 the set of all interior edges or flat faces. We denote by h_T the meshsize of $T \in \mathcal{T}_h$ and by $h = \max_{T \in \mathcal{T}_h} h_T$ the meshsize of \mathcal{T}_h .

Let $T \in \mathcal{T}_h$ be a polygonal or polyhedral region with boundary ∂T . With every element T we associate a product space $\mathcal{W}(T)$ defined as

$$W(T) := L^2(T) \times L^2(\partial T) \times L^2(\partial T).$$

The element of this space is denoted by $\{v_0, v_b, v_n\}$. Such definition is quite general, and just to give an example, if $v \in C^1(T)$ we can define v_0 to be just v, v_b to be the trace of v on ∂T ; $v_n = a\nabla v \cdot \mathbf{n}$ to be the trace of the flux on ∂T . Here \mathbf{n} is the outward normal vector on ∂T . In the most general case, the members of such triplet do not have to be related at all.

Given $v \in \mathcal{W}(T)$ (note v is a triplet of functions), we now define the functionals (distributions) $[\nabla_w v](\psi)$ and $[\mathcal{L}_w v](\phi)$ for all $\psi \in [H^1(T)]^d$, $\phi \in H^2(T)$ as follows:

$$\begin{split} [\nabla_w v](\boldsymbol{\psi})_T &:= -(v_0, \nabla \cdot \boldsymbol{\psi})_T + \langle v_b, \boldsymbol{\psi} \cdot \boldsymbol{n} \rangle_{\partial T}, \\ [\mathcal{L}_w v](\phi)_T &:= (v_0, \mathcal{L}\phi)_T - \langle v_b, a \nabla \phi \cdot \boldsymbol{n} \rangle_{\partial T} + \langle v_n, \phi \rangle_{\partial T}. \end{split}$$

Note that $\nabla_w v$ and $\mathcal{L}_w v$ are the distributional versions of ∇ and $\nabla \cdot (a\nabla)$, respectively.

We now define the discrete versions of these functionals. Let us denote by $P_r(T)$ the space of polynomials on T of degree $(\leq r)$. The discretizations of $[\nabla_w v]$ and $[\mathcal{L}_w v]$ for $v \in \mathcal{W}(T)$ are defined as the projections on $[P_r(T)]^d$ of the Riesz representation of $[\nabla_w](\cdot)$, and $[\mathcal{L}_w](\cdot)$. Namely, for all $\psi \in [P_r(T)]^d$, $w \in P_r(T)$, we set

$$(\nabla_{w,r,T}v,\boldsymbol{\psi})_T = [\nabla_w v](\boldsymbol{\psi}) = -(v_0, \nabla \cdot \boldsymbol{\psi})_T + \langle v_b, \boldsymbol{\psi} \cdot \boldsymbol{n} \rangle_{\partial T}, \tag{3.2}$$

$$(\mathcal{L}_{w,r,T}v, w)_T = [\mathcal{L}_{w,r,T}v](w) = (v_0, \mathcal{L}w)_T - \langle v_b, a\nabla w \cdot \mathbf{n} \rangle_{\partial T} + \langle v_n, w \rangle_{\partial T}.$$
(3.3)

Integration by parts gives the equivalent representations of these projections:

$$(\nabla_{w,r,T}v,\boldsymbol{\psi})_T = (\nabla v_0,\boldsymbol{\psi})_T - \langle v_0 - v_b,\boldsymbol{\psi}\cdot\boldsymbol{n}\rangle_{\partial T},\tag{3.4}$$

$$(\mathcal{L}_{w,r,T}v, w)_T = (\mathcal{L}v_0, w)_T + \langle v_0 - v_b, a\nabla w \cdot \mathbf{n} \rangle_{\partial T} - \langle a\nabla v_0 \cdot \mathbf{n} - v_n, w \rangle_{\partial T}. \tag{3.5}$$

4. Primal-dual weak Galerkin formulation

We now consider the following local and global piece-wise polynomial spaces (with and without boundary values). For a given integer $k \ge 1$ and $s \ge 0$ we define:

$$W_k(T) = P_k(T) \times P_k(\partial T) \times P_{k-1}(\partial T),$$

$$W_h = \left\{ \{\sigma_0, \sigma_b, \sigma_n\} : \{\sigma_0, \sigma_b, \sigma_n\} |_{T} \in W_k(T), \forall T \in \mathcal{T}_h \right\},$$

$$W_h^0 = \{v \in W_h : v_b = 0 \text{ on } \Gamma_D, v_n = 0 \text{ on } \Gamma_N \},$$

$$M_h = \{w : w |_{T} \in P_s(T), \forall T \in \mathcal{T}_h \}.$$

Here, the integer s is usually taken to be either k-1 or k-2. For any $\lambda \in W_h$, $w \in W_h$, and $u \in M_h$, we introduce the following bilinear forms

$$s(\lambda, w) = \sum_{T \in \mathcal{T}_h} s_T(\lambda, w), \tag{4.1}$$

$$b(u, w) = \sum_{T \in \mathcal{T}_h} (u, \mathcal{L}_w w + \mathbf{b} \cdot \nabla_w w)_T, \tag{4.2}$$

where

$$s_{T}(\lambda, w) = h_{T}^{-3} \langle (|a|_{T} + |\mathbf{b} \cdot \mathbf{n}|)(\lambda_{0} - \lambda_{b}), w_{0} - w_{b} \rangle_{\partial T}$$

$$+ h_{T}^{-1} \langle a \nabla \lambda_{0} \cdot \mathbf{n} - \lambda_{n}, a \nabla w_{0} \cdot \mathbf{n} - w_{n} \rangle_{\partial T}$$

$$+ \gamma (\mathcal{L}\lambda_{0} + \mathbf{b} \cdot \nabla \lambda_{0}, \mathcal{L}w_{0} + \mathbf{b} \cdot \nabla w_{0})_{T}.$$

$$(4.3)$$

Here, $\gamma \geq 0$ is a parameter independent of the meshsize h and the coefficients of the PDE; and $|a|_T^2 = \sup_{\mathbf{x} \in T} \left(\sum_{i,j=1}^d a_{ij}^2(\mathbf{x}) \right)$. With this setup and notation, the primal–dual weak Galerkin finite element method for the convection–diffusion model problem (1.1) is as follows:

Algorithm 4.1 (*Primal–Dual Weak Galerkin*). Find $(u_h; \lambda_h) \in M_h \times W_h^0$ satisfying

$$s(\lambda_h, w) + b(u_h, w) = -(f, w_0) + \langle g_2, w_b \rangle_{\Gamma_N} + \langle g_1, w_n \rangle_{\Gamma_D}, \quad \forall w \in W_h^0,$$

$$(4.4)$$

$$b(v, \lambda_h) = 0, \qquad \forall v \in M_h. \tag{4.5}$$

For any $w \in H^1(\Omega)$, denote by $Q_h w$ the L^2 projection onto the weak finite element space W_h such that on each element T.

$$Q_h w = \{Q_0 w, Q_b w, Q_n (a \nabla w \cdot \mathbf{n})\}.$$

Here and in what follows of this paper, on each element T, Q_0 denotes the L^2 projection operator onto $P_k(T)$; on each edge or face $e \subset \partial T$, Q_b and Q_n stand for the L^2 projection operators onto $P_k(e)$ and $P_{k-1}(e)$, respectively. We denote by Q_h^{k-1} and Q_h^s the L^2 projection operators onto the space of piecewise vector-valued polynomials of degree $\leq (k-1)$ and the space M_b , respectively.

Lemma 4.1. The L^2 projection operators Q_h , Q_h^{k-1} and Q_h^s satisfy the following commuting relations:

$$\nabla_w(Q_h w) = \mathcal{Q}_h^{k-1}(\nabla w), \qquad \forall w \in H^1(T); \tag{4.6}$$

$$\mathcal{L}_w(Q_h w) = \mathcal{Q}_h^s(\mathcal{L}w), \qquad \forall w \in H^1(T), \ a \nabla w \in H(\operatorname{div}; T). \tag{4.7}$$

Proof. The detailed proof of (4.6) can be found in [55].

As to (4.7), for any $\phi \in P_s(T)$ and $w \in H^1(T)$ such that $a\nabla w \in H(\text{div}; T)$, from (3.3) and integration by parts, we have

$$\begin{split} (\mathcal{L}_w(Q_h w), \phi)_T &= (Q_0 w, \mathcal{L}\phi)_T - \langle Q_b w, a \nabla \phi \cdot \mathbf{n} \rangle_{\partial T} + \langle Q_n(a \nabla w \cdot \mathbf{n}), \phi \rangle_{\partial T} \\ &= (w, \mathcal{L}\phi)_T - \langle w, a \nabla \phi \cdot \mathbf{n} \rangle_{\partial T} + \langle a \nabla w \cdot \mathbf{n}, \phi \rangle_{\partial T} \\ &= (\mathcal{L}w, \phi)_T = (\mathcal{Q}_b^s(\mathcal{L}w), \phi)_T, \end{split}$$

which completes the proof of (4.7). \square

5. Existence and uniqueness

The stabilizer $s(\cdot, \cdot)$ induces a semi-norm in the finite element space W_h as follows:

$$||w|| = s(w, w)^{\frac{1}{2}}, \quad \forall w \in W_h.$$
 (5.1)

In what follows of this paper, for the convenience of analysis, we assume that the convection vector \mathbf{b} and the diffusion tensor a are piecewise constants with respect to the partition \mathcal{T}_h . The analysis, however, can be generalized to the case that the convection \mathbf{b} and diffusion a are piecewise smooth functions.

Before we prove the existence and uniqueness (which follow from Lemma 5.2) we need the following result which is found in [55].

Lemma 5.1. Let \mathcal{T}_h be a shape regular partition of Ω . For $0 \le t \le \min(2, k)$, the following estimates hold true:

$$\sum_{T \in \mathcal{T}_{b}} h_{T}^{2t} \| u - Q_{0}u \|_{t,T}^{2} \lesssim h^{2(m+1)} \| u \|_{m+1}^{2}, \qquad m \in [t-1, k], \ k \ge 1,$$

$$(5.2)$$

$$\sum_{T \in \mathcal{T}_t} h_T^{2t} \| u - \mathcal{Q}_h^{(k-1)} u \|_{t,T}^2 \lesssim h^{2m} \| u \|_m^2, \qquad m \in [t, k], \ k \ge 1,$$
(5.3)

$$\sum_{T \in \mathcal{T}_{k}} h_{T}^{2t} \| u - \mathcal{Q}_{h}^{(k-2)} u \|_{t,T}^{2} \lesssim h^{2m} \| u \|_{m}^{2}, \qquad m \in [t, k-1], \ k \ge 2.$$
 (5.4)

We are ready to prove that the discrete problem is solvable. We have the following result.

Lemma 5.2. Assume the convection tensor \mathbf{b} and diffusion tensor a are uniformly piecewise constants with respect to the finite element partition \mathcal{T}_h . The following inf–sup condition holds true:

$$\sup_{\lambda \in W_h^0} \frac{b(v,\lambda)}{\|\lambda\|} \ge \beta_0 h^{\epsilon} \|v\|_{\epsilon}, \quad \forall v \in M_h, \tag{5.5}$$

where $\beta_0 > 0$ is a constant independent of the meshsize h.

Proof. For any $\psi \in H^{-\epsilon}(\Omega)$, let $w \in H^{2-\epsilon}(\Omega)$ be the solution to the dual problem (2.2) satisfying the regularity estimate (2.3). By letting $\rho = Q_h w \in W_h^0$, from the trace inequality (3.1) with $\theta = 0$, and the estimate (5.2), we arrive at

$$\sum_{T \in \mathcal{T}_{h}} h_{T}^{-3} \int_{\partial T} (|a|_{T} + |\mathbf{b} \cdot \mathbf{n}|) (\rho_{0} - \rho_{b})^{2} ds$$

$$\lesssim \sum_{T \in \mathcal{T}_{h}} h_{T}^{-3} \int_{\partial T} |Q_{0}w - Q_{b}w|^{2} ds$$

$$\lesssim \sum_{T \in \mathcal{T}_{h}} h_{T}^{-3} \int_{\partial T} |Q_{0}w - w|^{2} ds$$

$$\lesssim \sum_{T \in \mathcal{T}_{h}} h_{T}^{-4} \int_{T} |Q_{0}w - w|^{2} dT + h_{T}^{-2} \int_{T} |\nabla Q_{0}w - \nabla w|^{2} dT$$

$$\lesssim h^{-2\epsilon} \|w\|_{2-\epsilon}^{2}.$$

$$(5.6)$$

Analogously, we have from the trace inequality (3.1) with $\theta = \epsilon$ that

$$\sum_{T \in \mathcal{T}_{h}} h_{T}^{-1} \int_{\partial T} |a \nabla \rho_{0} \cdot \mathbf{n} - \rho_{n}|^{2} ds$$

$$\lesssim \sum_{T \in \mathcal{T}_{h}} h_{T}^{-1} \int_{\partial T} |a \nabla Q_{0} w \cdot \mathbf{n} - Q_{n} (a \nabla w \cdot \mathbf{n})|^{2} ds$$

$$\lesssim \sum_{T \in \mathcal{T}_{h}} h_{T}^{-1} \int_{\partial T} |a \nabla Q_{0} w \cdot \mathbf{n} - a \nabla w \cdot \mathbf{n}|^{2} ds$$

$$\lesssim \sum_{T \in \mathcal{T}_{h}} h_{T}^{-2} ||a \nabla Q_{0} w \cdot \mathbf{n} - a \nabla w \cdot \mathbf{n}||_{T}^{2} + h_{T}^{-2\epsilon} ||a \nabla Q_{0} w \cdot \mathbf{n} - a \nabla w \cdot \mathbf{n}||_{1-\epsilon, T}^{2}$$

$$\lesssim h^{-2\epsilon} ||w||_{2-\epsilon}^{2\epsilon}.$$
(5.7)

The inverse inequality then gives

$$\sum_{T \in \mathcal{T}_{h}} \gamma (\mathcal{L}\rho_{0} + \boldsymbol{b} \cdot \nabla \rho_{0}, \mathcal{L}\rho_{0} + \boldsymbol{b} \cdot \nabla \rho_{0})_{T} \lesssim \gamma \sum_{T \in \mathcal{T}_{h}} h_{T}^{-2\epsilon} \|\rho_{0}\|_{2-\epsilon, T}^{2}$$

$$\lesssim \gamma \sum_{T \in \mathcal{T}_{h}} h_{T}^{-2\epsilon} \|Q_{0}w\|_{2-\epsilon, T}^{2}$$

$$\lesssim \gamma h^{-2\epsilon} \|w\|_{2-\epsilon}^{2}.$$
(5.8)

By combining the estimates (5.6)–(5.8), the $H^{2-\epsilon}$ -regularity estimate (2.3), and the definition of $\|\rho\|$, we arrive at

$$\|\rho\| \lesssim h^{-\epsilon} \|\psi\|_{-\epsilon}. \tag{5.9}$$

Now, by letting $\rho = Q_h w \in W_h^0$, and then using Lemma 4.1 we obtain

$$b(v, \rho) = \sum_{T \in \mathcal{T}_h} (v, \mathcal{L}_w(Q_h w) + \boldsymbol{b} \cdot \nabla_w(Q_h w))_T$$

$$= \sum_{T \in \mathcal{T}_h} (v, \mathcal{Q}_h^s(\mathcal{L}w))_T + (\boldsymbol{b}v, \mathcal{Q}_h^{k-1}(\nabla w))_T$$

$$= \sum_{T \in \mathcal{T}_h} (v, \mathcal{L}w)_T + (\boldsymbol{b}v, \nabla w)_T$$

$$= \sum_{T \in \mathcal{T}_h} (v, \mathcal{L}w + \boldsymbol{b} \cdot \nabla w)_T$$

$$= (v, \psi).$$
(5.10)

Using (5.10) and (5.9) gives

$$\begin{split} \sup_{\lambda \in W_h^0} \frac{b(v,\lambda)}{\|\lambda\|} &\geq \sup_{\rho = Q_h w \in W_h^0} \frac{b(v,\rho)}{\|\rho\|} \\ &= \sup_{\psi \in H^{-\epsilon}(\Omega)} \frac{(v,\psi)}{\|\rho(\psi)\|} \\ &\geq \beta_0 \sup_{\psi \in H^{-\epsilon}(\Omega)} \frac{(v,\psi)}{h^{-\epsilon} \|\psi\|_{-\epsilon}} \\ &= \beta_0 h^{\epsilon} \|v\|_{\epsilon} \end{split}$$

for a constant β_0 independent of the meshsize h. This completes the proof of the lemma. \Box

Remark 5.1. If the stabilizer $s_T(\lambda, w)$ defined in (4.3) is chosen depending on the regularity as follows

$$s_{T}(\lambda, w) = h_{T}^{-3+2\epsilon} \langle (|a|_{T} + |\mathbf{b} \cdot \mathbf{n}|)(\lambda_{0} - \lambda_{b}), w_{0} - w_{b} \rangle_{\partial T}$$

$$+ h_{T}^{-1+2\epsilon} \langle a \nabla \lambda_{0} \cdot \mathbf{n} - \lambda_{n}, a \nabla w_{0} \cdot \mathbf{n} - w_{n} \rangle_{\partial T}$$

$$+ \gamma h_{T}^{2\epsilon} (\mathcal{L}\lambda_{0} + \mathbf{b} \cdot \nabla \lambda_{0}, \mathcal{L}w_{0} + \mathbf{b} \cdot \nabla w_{0})_{T},$$

then the inf-sup condition (5.5) is independent of h.

The following theorem is concerned with the main result on solution existence and uniqueness for the primal-dual weak Galerkin schemes (4.4)–(4.5).

Theorem 5.3. Assume that the diffusion tensor $a = a(\mathbf{x})$ and the convection vector \mathbf{b} are piecewise constants with respect to the finite element partition \mathcal{T}_h . Under the $H^{2-\epsilon}(0 \le \epsilon < \frac{1}{2})$ -regularity assumption (2.3), the primal-dual weak Galerkin finite element algorithm (4.4)–(4.5) has one and only one solution for any $k \ge 2$ and s = k - 2 or s = k - 1 when $\gamma > 0$. For the case of $\gamma = 0$ (i.e., no residual stability), the numerical scheme (4.4)–(4.5) has one and only one solution for any $k \ge 2$ and s = k - 1.

Proof. It suffices to show that zero is the only solution to the problems (4.4)–(4.5) with homogeneous data f=0, $g_1=0$ and $g_2=0$. To this end, assume f=0, $g_1=0$ and $g_2=0$ in (4.4)–(4.5). By letting $v=u_h$ and $w=\lambda_h$, the difference of (4.4) and (4.5) gives $s(\lambda_h, \lambda_h)=0$, which implies $\lambda_0=\lambda_b$ and $a\nabla\lambda_0\cdot \mathbf{n}=\lambda_n$ on each ∂T . This, together with the fact that $\lambda_h\in W_h^0$, leads to $\lambda_0=0$ on Γ_D and $a\nabla\lambda_0\cdot \mathbf{n}=0$ on Γ_N .

Next, it follows from (4.5), (3.4), (3.5) and integration by parts that for all $v \in M_h$

$$D = D(v, \lambda_h)$$

$$= \sum_{T \in \mathcal{T}_h} (v, \mathcal{L}_w \lambda_h + \mathbf{b} \cdot \nabla_w \lambda_h)_T$$

$$= \sum_{T \in \mathcal{T}_h} (\mathcal{L}\lambda_0, v)_T + \langle \lambda_0 - \lambda_b, a \nabla v \cdot \mathbf{n} \rangle_{\partial T} - \langle a \nabla \lambda_0 \cdot \mathbf{n} - \lambda_n, v \rangle_{\partial T}$$

$$+ (\nabla \lambda_0, \mathbf{b}v) - \langle \lambda_0 - \lambda_b, \mathbf{b}v \cdot \mathbf{n} \rangle_{\partial T}$$

$$= \sum_{T \in \mathcal{T}_h} (\mathcal{L}\lambda_0 + \mathbf{b} \cdot \nabla \lambda_0, v)_T + \langle \lambda_0 - \lambda_b, (a \nabla v - \mathbf{b}v) \cdot \mathbf{n} \rangle_{\partial T}$$

$$- \langle a \nabla \lambda_0 \cdot \mathbf{n} - \lambda_n, v \rangle_{\partial T}$$

$$= \sum_{T \in \mathcal{T}_h} (\mathcal{L}\lambda_0 + \mathbf{b} \cdot \nabla \lambda_0, v)_T,$$

$$(5.11)$$

where we have used $\lambda_0 = \lambda_b$ and $a \nabla \lambda_0 \cdot \boldsymbol{n} = \lambda_n$ on each ∂T . This implies $\mathcal{L}\lambda_0 + \boldsymbol{b} \cdot \nabla \lambda_0 = 0$ on each $T \in \mathcal{T}_h$ by taking $v = \mathcal{L}\lambda_0 + \boldsymbol{b} \cdot \nabla \lambda_0$ if s = k-1. For the case of s = k-2, from $\gamma > 0$ and the fact that $s(\lambda_h, \lambda_h) = 0$ we have $\mathcal{L}\lambda_0 + \boldsymbol{b} \cdot \nabla \lambda_0 = 0$ on each element $T \in \mathcal{T}_h$. Since $\lambda_0 = 0$ on Γ_D and $a \nabla \lambda_0 \cdot \boldsymbol{n} = 0$ on Γ_N , we then have $\lambda_0 \equiv 0$ in Ω . It follows that $\lambda_h \equiv 0$, as $\lambda_b = \lambda_0$ and $\lambda_n = a \nabla \lambda_0 \cdot \boldsymbol{n}$ on each ∂T .

To show that $u_h \equiv 0$, we use $\lambda_h \equiv 0$ and Eq. (4.4) to obtain

$$b(u_h, w) = 0, \qquad \forall w \in W_h^0. \tag{5.12}$$

From Lemma 5.2, we have

$$\sup_{w\in W_h^0}\frac{b(u_h,w)}{\|w\|}\geq \beta_0 h^{\epsilon}\|u_h\|_{\epsilon},$$

which, combined with (5.12), gives $u_h \equiv 0$ in Ω . This completes the proof of the theorem. \square

6. Error equations

Let u and $(u_h, \lambda_h) \in M_h \times W_h^0$ be the solution of (1.1) and its discretization schemes (4.4)–(4.5), respectively. Note that λ_h approximates the trivial function $\lambda = 0$ as the Lagrange multiplier.

Lemma 6.1. Assume that the diffusion tensor $a = a(\mathbf{x})$ and the convection vector \mathbf{b} are piecewise constant functions in Ω with respect to the finite element partition \mathcal{T}_h . For any $\sigma \in W_h$ and $v \in M_h$, the following identity holds true:

$$(\mathcal{L}_{w}\sigma + \boldsymbol{b} \cdot \nabla_{w}\sigma, v)_{T} = (\mathcal{L}\sigma_{0} + \boldsymbol{b} \cdot \nabla\sigma_{0}, v)_{T} + R_{T}(\sigma, v), \tag{6.1}$$

where

$$R_T(\sigma, v) = \langle \sigma_0 - \sigma_b, (a\nabla v - bv) \cdot \mathbf{n} \rangle_{\partial T} - \langle a\nabla \sigma_0 \cdot \mathbf{n} - \sigma_n, v \rangle_{\partial T}.$$

$$(6.2)$$

Proof. From (3.4) and (3.5), we have

$$\begin{aligned} & (\mathcal{L}_w \sigma + \boldsymbol{b} \cdot \nabla_w \sigma, v)_T \\ = & (\nabla_w \sigma, \boldsymbol{b} v)_T + (\mathcal{L}_w \sigma, v)_T \\ = & (\nabla \sigma_0, \boldsymbol{b} v) - \langle \sigma_0 - \sigma_b, \boldsymbol{b} v \cdot \boldsymbol{n} \rangle_{\partial T} + (\mathcal{L} \sigma_0, v)_T \\ & + \langle \sigma_0 - \sigma_b, a \nabla v \cdot \boldsymbol{n} \rangle_{\partial T} - \langle a \nabla \sigma_0 \cdot \boldsymbol{n} - \sigma_n, v \rangle_{\partial T} \\ = & (\mathcal{L} \sigma_0 + \boldsymbol{b} \cdot \nabla \sigma_0, v)_T + R_T(\sigma, v), \end{aligned}$$

where $R_T(\sigma, v)$ is given by (6.2). \square

By error functions we mean the difference between the numerical solution arising from (4.4)–(4.5) and the L^2 projection of the exact solution of (1.1); i.e.,

$$e_h = u_h - \mathcal{Q}_h^s u, \tag{6.3}$$

$$\varepsilon_h = \lambda_h - Q_h \lambda = \lambda_h. \tag{6.4}$$

Lemma 6.2. Let u and $(u_h; \lambda_h) \in M_h \times W_h^0$ be the solutions arising from (1.1) and (4.4)–(4.5), respectively. Assume that the diffusion tensor $a = a(\mathbf{x})$ and the convection vector \mathbf{b} are piecewise constant functions in Ω with respect to the finite element partition \mathcal{T}_h . Then, the error functions e_h and ε_h satisfy the following equations

$$s(\varepsilon_h, w) + b(e_h, w) = \ell_u(w), \qquad \forall \ w \in W_h^0, \tag{6.5}$$

$$b(v, \varepsilon_h) = 0, \qquad \forall v \in M_h, \tag{6.6}$$

where $\ell_u(w)$ is given by

$$\ell_{u}(w) = \sum_{T \in \mathcal{T}_{h}} (\mathcal{L}w_{0} + \boldsymbol{b} \cdot \nabla w_{0}, u - \mathcal{Q}_{h}^{s}u)_{T}$$

$$+ \langle w_{0} - w_{b}, (a\nabla(u - \mathcal{Q}_{h}^{s}u) - \boldsymbol{b}(u - \mathcal{Q}_{h}^{s}u)) \cdot \boldsymbol{n} \rangle_{\partial T}$$

$$- \langle a\nabla w_{0} \cdot \boldsymbol{n} - w_{n}, u - \mathcal{Q}_{h}^{s}u \rangle_{\partial T}.$$

$$(6.7)$$

Proof. From (6.4) and (4.5) we have

$$b(v, \varepsilon_h) = b(v, \lambda_h) = 0, \quad \forall v \in M_h,$$

which gives rise to (6.6).

Next, observe that $\lambda = 0$. Thus, from (4.4) we arrive at

$$s(\lambda_h - Q_h\lambda, w) + b(u_h - Q_h^s u, w)$$

$$= s(\lambda_h, w) + b(u_h, w) - b(Q_h^s u, w)$$

$$= -(f, w_0) + \langle g_2, w_b \rangle_{\Gamma_N} + \langle g_1, w_n \rangle_{\Gamma_D} - b(Q_h^s u, w).$$
(6.8)

For the term $b(Q_h^s u, w)$, we use Lemma 6.1 to obtain

$$b(\mathcal{Q}_{h}^{s}u, w)$$

$$= \sum_{T \in \mathcal{T}_{h}} (\mathcal{Q}_{h}^{s}u, \mathcal{L}_{w}w + \boldsymbol{b} \cdot \nabla_{w}w)_{T}$$

$$= \sum_{T \in \mathcal{T}_{h}} (\mathcal{L}w_{0} + \boldsymbol{b} \cdot \nabla w_{0}, \mathcal{Q}_{h}^{s}u)_{T} + R_{T}(w, \mathcal{Q}_{h}^{s}u)$$

$$= \sum_{T \in \mathcal{T}_{h}} (\mathcal{L}w_{0} + \boldsymbol{b} \cdot \nabla w_{0}, u)_{T} + (\mathcal{L}w_{0} + \boldsymbol{b} \cdot \nabla w_{0}, \mathcal{Q}_{h}^{s}u - u)_{T} + R_{T}(w, \mathcal{Q}_{h}^{s}u).$$

$$(6.9)$$

Integration by parts then shows that

$$\sum_{T \in \mathcal{T}_h} (\mathcal{L}w_0 + \boldsymbol{b} \cdot \nabla w_0, u)_T$$

$$= \sum_{T \in \mathcal{T}_h} (w_0, \nabla \cdot (a\nabla u - \boldsymbol{b}u))_T - \langle w_0, (a\nabla u - \boldsymbol{b}u) \cdot \boldsymbol{n} \rangle_{\partial T} + \langle a\nabla w_0 \cdot \boldsymbol{n}, u \rangle_{\partial T}.$$
(6.10)

Since u is the exact solution of (1.1), $w_b = 0$ on Γ_D and $w_n = 0$ on Γ_N , we have

$$\sum_{T \in \mathcal{T}_b} \langle w_b, (a \nabla u - \boldsymbol{b} u) \cdot \boldsymbol{n} \rangle_{\partial T} = -\langle w_b, g_2 \rangle_{\Gamma_N}, \tag{6.11}$$

$$\sum_{T \in \mathcal{T}_h} \langle w_n, u \rangle_{\partial T} = \langle w_n, g_1 \rangle_{\Gamma_D}. \tag{6.12}$$

Using (6.10), (6.11), (6.12) and (1.1), we arrive at

$$\sum_{T \in \mathcal{T}_{h}} (\mathcal{L}w_{0} + \boldsymbol{b} \cdot \nabla w_{0}, u)_{T}$$

$$= -(w_{0}, f) - \sum_{T \in \mathcal{T}_{h}} \langle w_{0} - w_{b}, (a\nabla u - \boldsymbol{b}u) \cdot \boldsymbol{n} \rangle_{\partial T} + \langle a\nabla w_{0} \cdot \boldsymbol{n} - w_{n}, u \rangle_{\partial T}$$

$$+ \langle w_{b}, g_{2} \rangle_{\Gamma_{N}} + \langle w_{n}, g_{1} \rangle_{\Gamma_{D}}.$$
(6.13)

Substituting (6.13) and (6.9) into (6.8) gives rise to the error equation (6.5), which completes the proof of the lemma. \Box

Remark 6.1. For C^0 -WG elements (i.e., $w_0 = w_b$ on the boundary of each element), the middle term in (6.7) vanishes so that $\ell_u(w)$ has the following simplified form:

$$\ell_{u}(w) = \sum_{T \in \mathcal{T}_{h}} (\mathcal{L}w_{0} + \boldsymbol{b} \cdot \nabla w_{0}, u - \mathcal{Q}_{h}^{s}u)_{T} - \langle a \nabla w_{0} \cdot \boldsymbol{n} - w_{n}, u - \mathcal{Q}_{h}^{s}u \rangle_{\partial T}, \tag{6.14}$$

which shall allow the derivation of an error estimate for the primal variable u_h with $u \in H^{\tau}(\Omega)$ for some $\tau < 1$.

7. Error estimates

For simplicity and without loss of generality we introduce a semi-norm $\|\cdot\|_b$ in the finite element space W_h . For any $v = \{v_0, v_h, v_n\} \in W_h$, define on each $T \in \mathcal{T}_h$

$$|||v|||_{b,T} := \langle (|a|_T + |\boldsymbol{b} \cdot \boldsymbol{n}|)(v_0 - v_b), v_0 - v_b \rangle_{\partial T}^{1/2}$$
(7.1)

and

$$|||v|||_b := \left(\sum_{T \in \mathcal{T}_h} h_T^{-3} |||v|||_{b,T}^2\right)^{\frac{1}{2}}.$$
(7.2)

It follows from (5.1), (4.1), and (4.3) that the following holds true:

$$\|v\|_h \le \|v\|, \qquad v \in W_h.$$
 (7.3)

We have the following main result.

Theorem 7.1. Let u be the solution of (1.1) and $(u_h, \lambda_h) \in M_h \times W_h^0$ be its numerical solution arising from (4.4)–(4.5) with index $k \ge 2$ and s = k - 2 or s = k - 1. Assume that the diffusion tensor $a = a(\mathbf{x})$ and the convection vector \mathbf{b} are piecewise constant functions in Ω with respect to the finite element partition \mathcal{T}_h which is shape regular [55]. Furthermore, assume that the exact solution u is sufficiently regular such that $u \in \prod_{T \in \mathcal{T}_h} H^{s+1}(T) \cap H^{2-\epsilon}(T)$ and that the regularity estimate (2.3) holds for the dual problem (2.2). Then, the following error estimate holds true:

$$\|\|\lambda_h\|\| + h^{\epsilon} \|e_h\|_{\epsilon} \lesssim \begin{cases} h^{s+2} (|a|^{\frac{1}{2}}h^{-1} + 1 + \delta_{s,k-2}\gamma^{-\frac{1}{2}}) \|\nabla^{s+1}u\|, & \text{if } s \geq 1, \\ h^2 (|a|^{\frac{1}{2}}h^{-1} + 1 + \gamma^{-\frac{1}{2}}) (\|\nabla u\| + h^{\frac{1}{2}-\epsilon} \|u\|_{2-\epsilon}), & \text{if } s = 0, \end{cases}$$

$$(7.4)$$

where $\delta_{i,j}$ is the Kronecker delta with value 1 when i = j and 0 otherwise.

Proof. We split the proof into several steps estimating the terms corresponding to each member of the triplet defining the errors. By letting $w = \varepsilon_h = \{\varepsilon_0, \varepsilon_h, \varepsilon_n\}$ in (6.5) and using (6.6) we arrive at

$$s(\varepsilon_h, \varepsilon_h) = \ell_u(\varepsilon_h),$$
 (7.5)

where, by (6.7),

$$\ell_{u}(\varepsilon_{h}) = \sum_{T \in \mathcal{T}_{h}} (\mathcal{L}\varepsilon_{0} + \boldsymbol{b} \cdot \nabla \varepsilon_{0}, u - \mathcal{Q}_{h}^{s}u)_{T}$$

$$+ \langle \varepsilon_{0} - \varepsilon_{b}, (a\nabla(u - \mathcal{Q}_{h}^{s}u) - \boldsymbol{b}(u - \mathcal{Q}_{h}^{s}u)) \cdot \boldsymbol{n} \rangle_{\partial T}$$

$$+ \langle \varepsilon_{n} - a\nabla\varepsilon_{0} \cdot \boldsymbol{n}, u - \mathcal{Q}_{h}^{s}u \rangle_{\partial T}$$

$$= \sum_{T \in \mathcal{T}_{h}} (J_{1}(T) + J_{2}(T) + J_{3}(T)).$$

$$(7.6)$$

Here $J_i(T)$ is given by the corresponding term in the summation formula for i = 1, 2, 3. The rest of the proof is focused on the estimate for each $J_i(T)$.

 $J_1(T)$ -estimate: We recall that s=k-2 or s=k-1 is the degree of polynomials for approximating the primal variable u. As $\mathcal{L}\varepsilon_0 + \boldsymbol{b} \cdot \nabla \varepsilon_0$ is a polynomial of degree k-1 on each element T, it follows that $J_1(T)=0$ when s=k-1. For the case of s=k-2, one may use the Cauchy–Schwarz inequality to obtain

$$\begin{aligned} |J_{1}(T)| &= \left| (\mathcal{L}\varepsilon_{0} + \boldsymbol{b} \cdot \nabla \varepsilon_{0}, u - \mathcal{Q}_{h}^{s} u)_{T} \right| \\ &\leq \left| (\mathcal{L}\varepsilon_{0} + \boldsymbol{b} \cdot \nabla \varepsilon_{0}, u - \mathcal{Q}_{h}^{s} u)_{T} \right| \\ &\leq \|\mathcal{L}\varepsilon_{0} + \boldsymbol{b} \cdot \nabla \varepsilon_{0}\|_{T} \|u - \mathcal{Q}_{h}^{s} u\|_{T} \\ &\leq h_{T}^{s+1} \|\nabla^{s+1} u\|_{T} \|\mathcal{L}\varepsilon_{0} + \boldsymbol{b} \cdot \nabla \varepsilon_{0}\|_{T}, \end{aligned}$$

$$(7.7)$$

where we have used the following interpolation error estimate in the last line:

$$\|u - \mathcal{Q}_{h}^{s}u\|_{T} \le Ch^{s+1}\|\nabla^{s+1}u\|_{T}. \tag{7.8}$$

By summing (7.7) over all $T \in \mathcal{T}_h$ we have from (5.1), (4.1), and (4.3) that

$$\sum_{T \in \mathcal{T}_h} |J_1(T)| \lesssim \begin{cases} \gamma^{-\frac{1}{2}} h^{s+1} \|\nabla^{s+1} u\| \|\varepsilon_h\|, & \text{for } s = k-2, \\ 0, & \text{for } s = k-1. \end{cases}$$
 (7.9)

 $J_2(T)$ -estimate: The Cauchy-Schwarz inequality and the boundedness of the convective vector **b** imply

$$|J_{2}(I)| = \left| \langle \varepsilon_{0} - \varepsilon_{b}, (a\nabla(u - \mathcal{Q}_{h}^{s}u) - \boldsymbol{b}(u - \mathcal{Q}_{h}^{s}u)) \cdot \boldsymbol{n} \rangle_{\partial T} \right|$$

$$\leq \left| \langle \varepsilon_{0} - \varepsilon_{b}, a\nabla(u - \mathcal{Q}_{h}^{s}u) \cdot \boldsymbol{n} \rangle_{\partial T} \right| + \left| \langle \varepsilon_{0} - \varepsilon_{b}, (u - \mathcal{Q}_{h}^{s}u)\boldsymbol{b} \cdot \boldsymbol{n} \rangle_{\partial T} \right|$$

$$\lesssim |a|_{T} \|\varepsilon_{0} - \varepsilon_{b}\|_{\partial T} \|\nabla(u - \mathcal{Q}_{h}^{s}u)\|_{\partial T} + \||\boldsymbol{b} \cdot \boldsymbol{n}|^{\frac{1}{2}} (\varepsilon_{0} - \varepsilon_{b})\|_{\partial T} \|u - \mathcal{Q}_{h}^{s}u\|_{\partial T}$$

$$\lesssim \left(|a|_{T}^{\frac{1}{2}} \|\nabla(u - \mathcal{Q}_{h}^{s}u)\|_{\partial T} + \|u - \mathcal{Q}_{h}^{s}u\|_{\partial T} \right) \|\varepsilon_{h}\|_{b,T}.$$

$$(7.10)$$

The boundary integral $\|u - \mathcal{Q}_{5}^{s}u\|_{\partial T}$ can be handled by using the trace inequality (3.1) and the estimate (7.8) as follows

$$\|u - Q_h^s u\|_{\partial T} \lesssim h_T^{s + \frac{1}{2}} \|\nabla^{s + 1} u\|_T. \tag{7.11}$$

As to the term $\|\nabla(u-\mathcal{Q}_h^s u)\|_{\partial T}$, for $s\geq 1$, from the error estimate for the L^2 projection $\mathcal{Q}_h^s u$ and the trace inequality (3.1) we have

$$\|\nabla(u - \mathcal{Q}_{h}^{s}u)\|_{\partial T} \lesssim h_{T}^{s-\frac{1}{2}} \|\nabla^{s+1}u\|_{T}. \tag{7.12}$$

For s=0, the above estimate must be modified by using the trace inequality (3.1) with $\theta=\epsilon$ as follows

$$\|\nabla(u - \mathcal{Q}_{h}^{s}u)\|_{\partial T} \lesssim h_{T}^{-\frac{1}{2}} \|\nabla u\|_{T} + h_{T}^{\frac{1}{2}-\epsilon} \|\nabla u\|_{1-\epsilon,T}. \tag{7.13}$$

Next, by substituting (7.11)–(7.13) into (7.10) we have

$$|J_{2}(T)| \lesssim \begin{cases} h_{T}^{s+\frac{1}{2}} (|a|_{T}^{\frac{1}{2}} h_{T}^{-1} + 1) \|\nabla^{s+1} u\|_{T} \|\varepsilon_{h}\|_{b,T}, & \text{for } s \geq 1, \\ h_{T}^{\frac{1}{2}} (|a|_{T}^{\frac{1}{2}} h_{T}^{-1} + 1) (\|\nabla u\|_{T} + h_{T}^{\frac{1}{2} - \epsilon} \|\nabla u\|_{1-\epsilon,T}) \|\varepsilon_{h}\|_{b,T}, & \text{for } s = 0, \end{cases}$$

Summing over $T \in \mathcal{T}_h$ and then using the Cauchy–Schwarz inequality and (7.2) gives

$$\sum_{T \in \mathcal{T}_h} |J_2(T)| \lesssim \begin{cases} h^{s+2} (|a|^{\frac{1}{2}} h^{-1} + 1) \|\nabla^{s+1} u\| \|\varepsilon_h\|_b, & \text{if } s \ge 1, \\ h^2 (|a|^{\frac{1}{2}} h^{-1} + 1) (\|\nabla u\| + h^{\frac{1}{2} - \epsilon} \|u\|_{2 - \epsilon}) \|\varepsilon_h\|_b, & \text{if } s = 0. \end{cases}$$

$$(7.14)$$

 $I_3(T)$ -estimate: From the Cauchy-Schwarz and the trace inequality (3.1) we obtain

$$\begin{aligned} |J_{3}(T)| &= \left| \langle \varepsilon_{n} - a \nabla \varepsilon_{0} \cdot \boldsymbol{n}, u - \mathcal{Q}_{h}^{s} u \rangle_{\partial T} \right| \\ &\leq \|\varepsilon_{n} - a \nabla \varepsilon_{0} \cdot \boldsymbol{n}\|_{\partial T} \|u - \mathcal{Q}_{h}^{s} u\|_{\partial T} \\ &\lesssim \|\varepsilon_{n} - a \nabla \varepsilon_{0} \cdot \boldsymbol{n}\|_{\partial T} \left(h_{T}^{-1} \|u - \mathcal{Q}_{h}^{s} u\|_{T}^{2} + h_{T} \|\nabla (u - \mathcal{Q}_{h}^{s} u)\|_{T}^{2} \right)^{1/2} \\ &\lesssim h_{T}^{s+\frac{1}{2}} \|\varepsilon_{n} - a \nabla \varepsilon_{0} \cdot \boldsymbol{n}\|_{\partial T} \|\nabla^{s+1} u\|_{T}. \end{aligned}$$

$$(7.15)$$

Summing over all the element $T \in \mathcal{T}_h$ yields

$$\sum_{T \in \mathcal{T}_{h}} |J_{3}(T)| \lesssim \sum_{T \in \mathcal{T}_{h}} h_{T}^{s+\frac{1}{2}} \|\varepsilon_{n} - a\nabla\varepsilon_{0} \cdot \boldsymbol{n}\|_{\partial T} \|\nabla^{s+1}u\|_{T}$$

$$\lesssim h^{s+1} \|\nabla^{s+1}u\| \left(\sum_{T \in \mathcal{T}_{h}} h_{T}^{-1} \|\varepsilon_{n} - a\nabla\varepsilon_{0} \cdot \boldsymbol{n}\|_{\partial T}^{2}\right)^{1/2}$$

$$\lesssim h^{s+1} \|\nabla^{s+1}u\| \|\varepsilon_{h}\|_{L}.$$

$$(7.16)$$

By combining (7.6) with the estimates (7.9), (7.14), and (7.16) we arrive at

$$|\ell_u(\varepsilon_h)| \lesssim \begin{cases} h^{s+2}(|a|^{\frac{1}{2}}h^{-1} + 1 + \delta_{s,k-2}\gamma^{-\frac{1}{2}})\|\nabla^{s+1}u\|\|\varepsilon_h\|, & \text{for } s \geq 1, \\ h^2(|a|^{\frac{1}{2}}h^{-1} + 1 + \gamma^{-\frac{1}{2}})(\|\nabla u\| + h^{\frac{1}{2}-\epsilon}\|u\|_{2-\epsilon})\|\varepsilon_h\|, & \text{for } s = 0, \end{cases}$$

where $\delta_{i,j}$ is the Kronecker delta with value 1 for i=j and 0 otherwise. Substituting the above estimate into (7.5) yields

$$\|\|\varepsilon_h\|\|^2 \lesssim \begin{cases} h^{s+2}(|a|^{\frac{1}{2}}h^{-1} + 1 + \delta_{s,k-2}\gamma^{-\frac{1}{2}})\|\nabla^{s+1}u\|\|\varepsilon_h\|, & \text{for } s \geq 1, \\ h^2(|a|^{\frac{1}{2}}h^{-1} + 1 + \gamma^{-\frac{1}{2}})(\|\nabla u\| + h^{\frac{1}{2}-\epsilon}\|u\|_{2-\epsilon})\|\varepsilon_h\|, & \text{for } s = 0, \end{cases}$$

which leads to

$$\|\|\varepsilon_{h}\|\| \lesssim \begin{cases} h^{s+2}(|a|^{\frac{1}{2}}h^{-1} + 1 + \delta_{s,k-2}\gamma^{-\frac{1}{2}})\|\nabla^{s+1}u\|, & \text{for } s \geq 1, \\ h^{2}(|a|^{\frac{1}{2}}h^{-1} + 1 + \gamma^{-\frac{1}{2}})(\|\nabla u\| + h^{\frac{1}{2}-\epsilon}\|u\|_{2-\epsilon}), & \text{for } s = 0. \end{cases}$$

$$(7.17)$$

Furthermore, the error equation (6.5) yields

$$b(e_h, w) = \ell_u(w) - s(\varepsilon_h, w), \quad \forall w \in W_h^0.$$

It follows that

for all $w \in W_h^0$. Thus, from the *inf-sup* condition (5.5) we obtain

$$\beta_0 h^{\epsilon} \|e_h\|_{\epsilon} \lesssim \begin{cases} h^{s+2} (|a|^{\frac{1}{2}}h^{-1} + 1 + \delta_{s,k-2}\gamma^{-\frac{1}{2}}) \|\nabla^{s+1}u\|, & \text{for } s \geq 1, \\ h^2 (|a|^{\frac{1}{2}}h^{-1} + 1 + \gamma^{-\frac{1}{2}}) (\|\nabla u\| + h^{\frac{1}{2}-\epsilon}\|u\|_{2-\epsilon}), & \text{for } s = 0, \end{cases}$$

which, together with the error estimate (7.17), completes the proof of the theorem. \Box

The triangle inequality and the error estimate (7.4) give the following for the numerical approximation of the primal variable.

Corollary 7.2. Under the assumptions of Theorem 7.1, one has the following optimal order error estimate in the H^{ϵ} -norm for $\epsilon \in [0, \frac{1}{2})$:

$$h^{\epsilon} \|u - u_h\|_{\epsilon} \lesssim \begin{cases} h^{s+2} (|a|^{\frac{1}{2}}h^{-1} + 1 + \delta_{s,k-2}\gamma^{-\frac{1}{2}}) \|\nabla^{s+1}u\|, & \text{if } s \geq 1, \\ h^2 (|a|^{\frac{1}{2}}h^{-1} + 1 + \gamma^{-\frac{1}{2}}) (\|\nabla u\| + h^{\frac{1}{2}-\epsilon} \|u\|_{2-\epsilon}), & \text{if } s = 0. \end{cases}$$

We emphasize that for s = k - 1 one has $(\mathcal{L}\varepsilon_0 + \boldsymbol{b} \cdot \nabla \varepsilon_0, u - \mathcal{Q}_h^s u)_T = 0$. The proof of Theorem 7.1 indicates that the following term

$$\gamma \int_{T} (\mathcal{L}\lambda_{0} + \boldsymbol{b} \cdot \nabla \lambda_{0}) (\mathcal{L}w_{0} + \boldsymbol{b} \cdot \nabla w_{0}) dT$$

in the stabilizer $s_T(\cdot, \cdot)$ (4.3) is no longer needed in the PDWG numerical schemes (4.4)–(4.5). The corresponding error estimate can be stated as follows:

$$h^{\epsilon} \|u - u_h\|_{\epsilon} \lesssim \begin{cases} h^{s+2} (|a|^{\frac{1}{2}}h^{-1} + 1) \|\nabla^{s+1}u\|, & \text{if } s \geq 1, \\ h^{2} (|a|^{\frac{1}{2}}h^{-1} + 1 + \gamma^{-\frac{1}{2}}) (\|\nabla u\| + h^{\frac{1}{2} - \epsilon} \|u\|_{2 - \epsilon}), & \text{if } s = 0. \end{cases}$$

8. Numerical results

This section shall report a variety of numerical results for the primal-dual weak Galerkin finite element schemes (4.4)–(4.5) of the lowest order; i.e., k = 2 and s = 0, 1. Our finite element partition \mathcal{T}_h is given through a successive uniform refinement of a coarse triangulation of the domain by dividing each coarse level triangular element into four congruent sub-triangles by connecting the three mid-points on its edge.

Both convex and non-convex polygonal domains are considered in the numerical experiments. The representatives of the convex domains are two squares $\Omega_1=(0,1)^2$ and $\Omega_3=(-1,1)^2$. The non-convex domains are featured by three examples: (i) the L-shaped domain Ω_2 with vertices $A_1=(0,0)$, $A_2=(2,0)$, $A_3=(2,1)$, $A_4=(1,1)$, $A_5=(1,2)$, and $A_6=(0,2)$; (ii) the cracked square domain $\Omega_4=(-1,1)^2\setminus(0,1)\times0$ (i.e., a crack along the edge $(0,1)\times0$); and (iii) the L-shaped domain Ω_5 with vertices $B_1=(-1,-1)$, $B_2=(1,-1)$, $B_3=(1,0)$, $B_4=(0,0)$, $B_5=(0,1)$, and $B_6=(-1,1)$.

The numerical method is based on the following configuration of the weak finite element space

$$W_{h,2} = {\lambda_h = {\lambda_0, \lambda_h, \lambda_n} : \lambda_0 \in P_2(T), \lambda_h \in P_2(e), \lambda_n \in P_1(e), e \subset \partial T, T \in \mathcal{T}_h},$$

and the finite element space

$$M_{h,s} = \{u_h : u_h|_T \in P_s(T), \ \forall T \in \mathcal{T}_h\}, \quad s = 0 \text{ or } 1.$$

The weak finite element space $W_{h,k}$ is said to be of C^0 -type if for any $v = \{v_0, v_b, v_n\} \in W_{h,k}$, one has $v_b = v_0|_{\partial T}$ on each element $T \in \mathcal{T}_h$. Likewise, C^{-1} -type elements are defined as the general case of $v = \{v_0, v_b, v_n\} \in W_{h,k}$ for which v_b is completely independent of v_0 on the edge of each element. It is clear that C^0 -type elements involve fewer degrees of freedom compared with the C^{-1} -type elements. But C^{-1} -type elements have the flexibility in element construction and approximation. It should be noted that, for C^{-1} -type elements, the unknowns associated with v_0 can be eliminated locally on each element in parallel through a condensation algorithm before assembling the global stiffness matrix.

For simplicity of implementation, our numerical experiments will be focused on C^0 -type elements; i.e., $\lambda_b = \lambda_0$ on ∂T for each element $T \in \mathcal{T}_h$. For convenience, the C^0 -type WG element with s = 1 (i.e., $M_{h,1}$) and s = 0 (i.e., $M_{h,0}$) will be

Table 8.1 Numerical rates of convergence for the $C^{-1} - P_2(T)/P_2(\partial T)/P_1(\partial T)/P_3(T)$ element with exact solution $u = \sin(x)\sin(y)$ on Ω_1 ; uniform triangular partitions; the diffusion tensor $a = \frac{1}{2}[1 + x^2, 0; 0, 1 + y^2]$; the convection vector $\mathbf{b} = [1, 1]'$; the stabilizer parameter $\gamma = 1$; full Dirichlet boundary condition

	1/h	$\ \lambda_h\ _0$	Order	$\ \lambda_b\ _0$	Order	$\ \lambda_h\ _1$	Order	$\ e_h\ _0$	Order
	1	0.06154		0.07356		0.2582		0.2576	
	2	0.006173	3.317	0.006173	3.575	0.04388	2.5575	0.08868	1.538
s = 1	4	0.0004702	3.715	0.0005948	3.375	0.004971	3.142	0.02248	1.980
	8	3.051E-05	3.946	3.847E-05	3.951	0.0005405	3.201	0.005592	2.007
	16	1.931E-06	3.982	2.431E-06	3.984	6.300E-05	3.101	0.0013957	2.002
	32	1.215E-07	3.991	1.528E-07	3.992	7.682E-06	3.036	0.0003488	2.000
	1/h	$\ \lambda_h\ _0$	Order	$\ \lambda_b\ _0$	Order	$\ \lambda_h\ _1$	Order	$\ e_h\ _0$	Order
	1	0.2081		0.1999		1.640		0.1353	
s = 0	2	0.04310	2.272	0.05059	1.983	0.4799	1.773	0.05270	1.3600
	4	0.006967	2.629	0.008601	2.556	0.1163	2.045	0.01998	1.399
	8	0.001193	2.546	0.001566	2.458	0.02810	2.049	0.008344	1.260
	16	0.0002439	2.290	0.0003357	2.222	0.006918	2.022	0.003852	1.115
	32	5.663 E-05	2.107	7.946E-05	2.079	0.001718	2.009	0.001881	1.034

denoted as C^0 - $P_2(T)/P_1(\partial T)/P_1(T)$ and C^0 - $P_2(T)/P_1(\partial T)/P_0(T)$ respectively. Analogously, the C^{-1} -type WG element with s=1 and s=0 will be denoted as C^{-1} - $P_2(T)/P_2(\partial T)/P_1(\partial T)/P$

Let $\lambda_h = \{\lambda_0, \lambda_b, \lambda_n\} \in W_{h,2}$ and $u_h \in M_{h,s}$ (s = 0, 1) be the numerical solutions arising from (4.4)–(4.5). To demonstrate the performance of the numerical method, the numerical solutions are compared with some appropriately-chosen interpolations of the exact solution u and λ in various norms. In particular, the primal variable u_h is compared with the exact solution u on each element at either the three vertices (for s = 1) or the center (for s = 0) – known as the nodal point interpolation $I_h u$. The auxiliary variable λ_h approximates the true solution $\lambda = 0$, and is compared with $Q_h \lambda = 0$. Thus, the error functions are respectively denoted by

$$\varepsilon_h = \lambda_h - Q_h \lambda \equiv {\{\lambda_0, \lambda_b, \lambda_n\}}, \quad e_h = u_h - I_h u.$$

The following norms are used to measure the error functions:

$$||e_h||_0 = \left(\sum_{T \in \mathcal{T}_h} \int_T e_h^2 dT\right)^{\frac{1}{2}}, |||\lambda_h|||_0 = \left(\sum_{T \in \mathcal{T}_h} \int_T \lambda_0^2 dT\right)^{\frac{1}{2}},$$

$$\|\|\lambda_b\|\|_0 = \left(\sum_{T \in \mathcal{T}_b} h_T \int_{\partial T} \lambda_b^2 ds\right)^{\frac{1}{2}}, \|\|\lambda_h\|\|_1 = \left(\sum_{T \in \mathcal{T}_b} h_T \int_{\partial T} \lambda_n^2 ds\right)^{\frac{1}{2}}.$$

Table 8.1 illustrates the performance of the PDWG finite element scheme for the test problem (1.1) when the C^{-1} -type $P_2(T)/P_2(\partial T)/P_1(\partial T)/P_1(\partial T)/P_1(\partial T)/P_1(T)$ element and the C^{-1} -type $P_2(T)/P_2(\partial T)/P_1(\partial T)/P_0(T)$ element are applied respectively. The configuration of this test problem is as follows: the domain is the unit square $\Omega_1 = (0, 1)^2$; the exact solution is $u = \sin(x)\sin(y)$; the diffusion tensor is $a(x) = \frac{1}{2}[1 + x^2, 0; 0, 1 + y^2]$; the convection vector is $\mathbf{b} = [1, 1]'$ and the stabilizer parameter $\gamma = 1$. We observe from Table 8.1 that the convergence rate for e_h in the L^2 norm is of an expected optimal order $\mathcal{O}(h^2)$ and $\mathcal{O}(h)$ for the C^{-1} - $P_2(T)/P_2(\partial T)/P_1(\partial T)/P_s(T)$ element on the uniform triangular partitions when s = 1 and s = 0 are employed respectively.

Tables 8.2–8.3 illustrate the performance of the PDWG finite element scheme for the test problem (1.1) when the exact solution is given by $u=\sin(x)\cos(y)$ for the C^0 -type $P_2(T)/P_1(\partial T)/P_1(T)$ element on the unit square domain Ω_1 and the L-shaped domain Ω_2 with stabilizer parameter $\gamma=0$. The diffusion tensor in (1.1) is given by $a=[10^{-10},0;0,10^{-10}]$ and the convection tensor by $\boldsymbol{b}=[1,1]$ which makes it a convection-dominated diffusion problem. The right-hand side function f, the Dirichlet boundary data g_1 , and the Neumann boundary data g_2 are chosen to match the exact solution u. The numerical results in Tables 8.2–8.3 show that the convergence rates for the error function e_h are of order r=2 in the discrete L^2 -norm on both the unit square domain Ω_1 and the L-shaped domain Ω_2 . The numerical results are in great consistency with the theoretical rate of convergence for e_h in the discrete L^2 -norm on the convex domain Ω_1 . The computational results for the non-convex domain Ω_2 outperform the theory shown in the previous section.

Table 8.4 illustrates the performance of the PDWG method with the C^0 - $P_2(T)/P_1(\partial T)/P_0(T)$ element when the exact solution is $u = \sin(x)\sin(y)$ on the domain Ω_1 . The diffusion tensor is given by $a = [1 + x^2 + y^2, 0; 0, 1 + x^2 + y^2]$ and the convection vector by $\mathbf{b} = [x, y]$. The stabilizer parameter is $\gamma = 0$. The convergence for e_h in the discrete L^2 norm is at the rate of $\mathcal{O}(h)$ which is consistent with what the theory predicts.

Tables 8.5–8.6 show the numerical results on the unit square domain Ω_1 for the C^0 - $P_2(T)/P_1(\partial T)/P_1(T)$ and C^0 - $P_2(T)/P_1(\partial T)/P_0(T)$ elements, respectively. In this numerical experiment, we consider a convection-dominated diffusion problem by taking the diffusion tensor as $a = [10^{-5}, 0; 0, 10^{-5}]$ and the convection vector $\mathbf{b} = [1, 0]$. The stabilizer parameter for the third term is given by $\gamma = 0$; and Dirichlet boundary data is imposed on all the boundary edges. The

Table 8.2 Numerical rates of convergence for the C^0 - $P_2(T)/P_1(\partial T)/P_1(T)$ element with exact solution $u = \sin(x)\cos(y)$ on $\Omega_1 = (0, 1)^2$; the diffusion tensor $a = [10^{-10}, 0; 0, 10^{-10}]$; the convection vector $\mathbf{b} = [1, 1]$; the stabilizer parameter $\gamma = 0$; Neumann boundary condition on the boundary edge $(0, 1) \times \{0\}$ and Dirichlet boundary condition on other three boundary edges.

1/h	$\ \lambda_h\ _0$	Order	$\ \lambda_h\ _1$	Order	$\ e_h\ _0$	Order
1	2.63E-13		0.005393		0.07722	
2	6.61E - 14	1.991	0.001270	2.087	0.02388	1.693
4	1.16E-14	2.514	1.58E-04	3.009	0.005821	2.036
8	1.69E-15	2.776	1.52E-05	3.378	0.001425	2.030
16	2.54E-16	2.731	1.33E-06	3.514	3.55E-04	2.005
32	3.66E-17	2.798	1.14E-07	3.538	8.89E-05	1.998

Table 8.3 Numerical rates of convergence for the C^0 - $P_2(T)/P_1(\partial T)/P_1(T)$ element with exact solution $u = \sin(x)\cos(y)$ on the L-shaped domain Ω_2 ; the diffusion tensor $a = [10^{-10}, 0; 0, 10^{-10}]$; the convection vector $\mathbf{b} = [1, 1]$; the stabilizer parameter $\gamma = 0$; Neumann boundary condition on the boundary edge $(0, 1) \times \{0\}$ and Dirichlet boundary condition on other boundary edges.

1/h	$\ \lambda_h\ _0$	Order	$\ \lambda_h\ _1$	Order	$\ e_h\ _0$	Order
1	2.81E-12		0.03304		0.2771	
2	5.91E-13	2.249	0.004297	2.943	0.06903	2.005
4	8.11E-14	2.866	4.49E - 04	3.260	0.01629	2.083
8	1.18E-14	2.780	4.25E-05	3.400	0.003996	2.028
16	2.12E-15	2.481	3.92E-06	3.437	9.92E - 04	2.010

Table 8.4 Numerical rates of convergence for the C^0 - $P_2(T)/P_1(\partial T)/P_0(T)$ element with exact solution $u = \sin(x)\sin(y)$ on Ω_1 ; the diffusion tensor $a = [1 + x^2 + y^2, 0; 0, 1 + x^2 + y^2]$; the convection vector $\mathbf{b} = [x, y]$; the stabilizer parameter $\gamma = 0$; full Dirichlet boundary condition.

1/h	$\ \lambda_h\ _0$	Order	$\ \lambda_h\ _1$	Order	$\ e_h\ _0$	Order
1	0.02967		0.4979		0.04851	
2	0.002843	3.384	0.1173	2.086	0.02801	0.7925
4	4.53E-04	2.649	0.02797	2.069	0.01272	1.138
8	1.02E-04	2.155	0.006792	2.042	0.006047	1.073
16	2.45E-05	2.053	0.001671	2.023	0.002980	1.021
32	6.07E-06	2.016	4.14E-04	2.012	0.001485	1.005

Table 8.5 Numerical rates of convergence for the C^0 - $P_2(T)/P_1(\partial T)/P_0(T)$ element with exact solution $u = 0.5(1 - \tanh((x - 0.5)/0.05))$ on Ω_1 ; the diffusion tensor $a = [10^{-5}, 0; 0, 10^{-5}]$; the convection vector $\mathbf{b} = [1, 0]$; the stabilizer parameter $\gamma = 0$; full Dirichlet boundary condition.

1/h	$\ \lambda_h\ _0$	Order	$\ \lambda_h\ _1$	Order	$\ e_h\ _0$	Order
1	1.32E-10		7.02E-06		0.06502	
2	1.01E-04	-19.54	1.66E-03	-7.882	57.82	-9.796
4	1.86E-05	2.442	6.28E-04	1.399	29.78	0.9571
8	2.61E-06	2.833	1.80E-04	1.803	6.781	2.135
16	2.32E-07	3.488	3.24E-05	2.476	1.725	1.975
32	1.54E-08	3.913	4.32E-06	2.906	0.4000	2.109

Table 8.6 Numerical rates of convergence for the C^0 - $P_2(T)/P_1(\partial T)/P_1(T)$ element with exact solution $u = 0.5(1 - \tanh((x - 0.5)/0.05))$ on Ω_1 ; the diffusion tensor $a = [10^{-5}, 0; 0, 10^{-5}]$; the convection vector $\mathbf{b} = [1, 0]$; the stabilizer parameter $\gamma = 0$; full Dirichlet boundary conditions.

1/h	$\ \lambda_h\ _0$	Order	$\ \lambda_h\ _1$	Order	$\ e_h\ _0$	Order
1	6.49E-06		0.3685		0.6662	
2	6.84E-07	3.246	0.07008	2.394	0.6305	0.07942
4	2.24E-07	1.614	0.01776	1.980	0.3130	1.010
8	4.12E-08	2.439	0.003311	2.423	0.1281	1.289
16	5.98E-09	2.785	3.58E-04	3.209	0.03184	2.009
32	1.23E-09	2.279	2.81E-05	3.671	0.006791	2.229

exact solution is $u = 0.5(1 - \tanh((x - 0.5)/0.05))$. The numerical results in Table 8.5 indicate that the convergence for e_h in the L^2 norm seem to arrive at a superconvergence rate of $\mathcal{O}(h^2)$ which is higher than the theoretical prediction of $\mathcal{O}(h)$ for the C^0 - $P_2(T)/P_1(\partial T)/P_0(T)$ element. Table 8.6 shows that the convergence for e_h in the L^2 norm is at the rate of $\mathcal{O}(h^2)$ for the C^0 - $P_2(T)/P_1(\partial T)/P_1(T)$ element which is consistent with the theoretical error estimate.

Tables 8.7–8.8 illustrate the numerical results for the C^0 - $P_2(T)/P_1(\partial T)/P_1(T)$ and the C^0 - $P_2(T)/P_1(\partial T)/P_0(T)$ elements on the unit square domain Ω_1 with exact solution $u = e^{-(x-0.5)^2/0.2-3(y-0.5)^2/0.2}$. The test problem has the diffusion tensor $a = [10^{-5}, 0; 0, 10^{-5}]$ and the convection $\mathbf{b} = [1, 0]$. The stabilizer parameters are chosen as $\gamma = 1$ and $\gamma = 0$,

Table 8.7 Numerical rates of convergence for the C^0 - $P_2(T)/P_1(\partial T)/P_0(T)$ element with exact solution $u = e^{-(x-0.5)^2/0.2-3(y-0.5)^2/0.2}$ on Ω_1 ; the diffusion tensor $a = [10^{-5}, 0; 0, 10^{-5}]$; the convection vector $\mathbf{b} = [1, 0]$; the stabilizer parameter $\gamma = 1$; Dirichlet boundary condition on the entire boundary.

1/h	$\ \lambda_h\ _0$	Order	$\ \lambda_h\ _1$	Order	$\ e_h\ _0$	Order
1	4.06E-15		8.77E-07		0.4682	
2	3.21E-04	-36.20	0.005274	-12.55	1.21E+02	-8.016
4	2.52E-05	3.673	7.73E-04	2.771	7.002	4.113
8	1.35E-06	4.221	9.47E-05	3.029	3.980	0.8152
16	8.44E-08	4.000	1.19E-05	2.998	0.8133	2.291
32	5.26E-09	4.004	1.48E-06	3.005	0.1313	2.631

Table 8.8 Numerical rates of convergence for the C^0 - $P_2(T)/P_1(\partial T)/P_1(T)$ element with exact solution $u = e^{-(x-0.5)^2/0.2-3(y-0.5)^2/0.2}$ on Ω_1 ; the diffusion tensor $a = [10^{-5}, 0; 0, 10^{-5}]$; the convection $\mathbf{b} = [1, 0]$; the stabilizer parameter $\gamma = 0$; Dirichlet boundary condition on the entire boundary.

1/h	$\ \lambda_h\ _0$	Order	$\ \lambda_h\ _1$	Order	$\ e_h\ _0$	Order
1	2.80E-10		0.05239		0.2339	
2	3.74E-07	-10.38	0.01817	1.528	0.1609	0.5398
4	7.24E-08	2.369	0.003381	2.426	0.1146	0.4893
8	1.77E-08	2.035	3.09E-04	3.452	0.03390	1.757
16	4.43E-09	1.994	2.93E-05	3.398	0.008362	2.019
32	1.27E-09	1.799	3.30E-06	3.151	0.002117	1.982

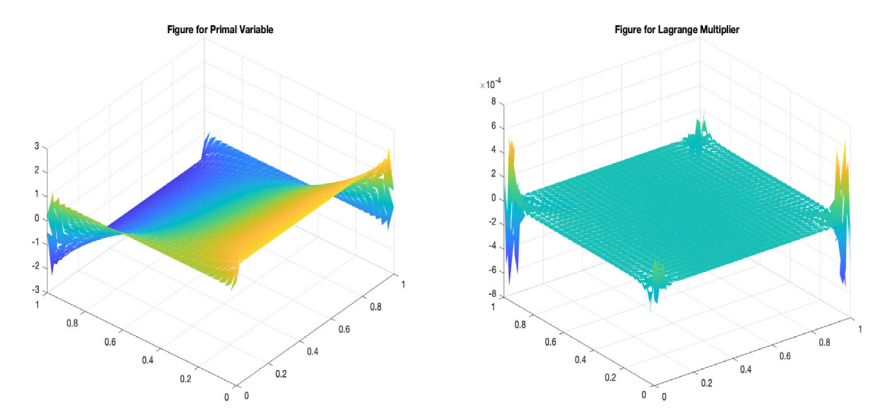


Fig. 8.1. Surface plots for the C^{-1} - $P_2(T)/P_2(\partial T)/P_1(\partial T)/P_1(T)$ element on the unit square domain Ω_1 ; left for the primal variable u_h ; right for the dual variable λ_0 .

respectively. The Dirichlet boundary condition is imposed on the entire boundary. The numerical results in Table 8.7 show a superconvergence for e_h in the L^2 norm, as the optimal order error estimate would imply a convergence at the rate of $\mathcal{O}(h)$ when the C^0 - $P_2(T)/P_1(\partial T)/P_0(T)$ element is used. Table 8.8 indicates that the convergence order for e_h in the discrete L^2 norm is consistent with what the theory predicts.

Figs. 8.1–8.2 illustrate the plots of the numerical solution u_h and the Lagrange multiplier λ_0 arising from the PDWG schemes (4.4)–(4.5) on the unit square domain Ω_1 . The diffusion tensor is a=[3/2,0;0,5], the convection vector is $\boldsymbol{b}=[1,1]$, and the load function is f=0. The full Dirichlet boundary data is set as follows: $g_1=1$ on the boundary edge 0*(0,1), $g_1=-1$ on the boundary edge 1*(0,1), $g_1=2$ on the boundary edge (0,1)*0, and $g_1=-2$ on the boundary edge (0,1)*1. Figs. 8.1–8.2 show the numerical solution u_h and the Lagrange multiplier λ_0 when the C^{-1} -type $P_2(T)/P_2(\partial T)/P_1(\partial T)/$

Fig. 8.5 illustrates the plots of the numerical solution u_h arising from the PDWG schemes (4.4)–(4.5) for a convection-dominated diffusion problem on the unit square domain Ω_1 . In this numerical experiment, the diffusion tensor is given by $a = [10^{-5}, 0; 0, 10^{-5}]$, the convection vector by $\mathbf{b} = [1, 0]$, and the load function is given by f = 1. The Neumann boundary data $g_2 = 10^{-5}$ is imposed on the boundary edge $\{0\} \times (0, 1)$, and the Dirichlet boundary data $g_1 = x$ is imposed on the rest of the boundary edges. The figure on the left shows the numerical solution u_h when the C^0 -type $P_2(T)/P_1(\partial T)/P_1(T)$

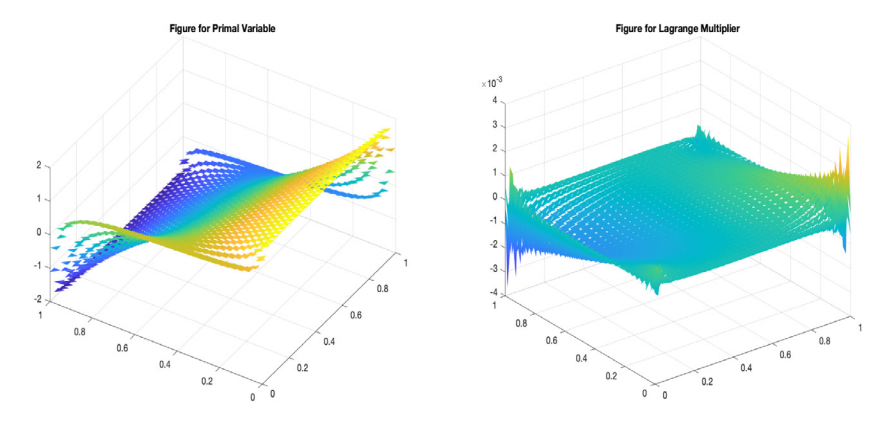


Fig. 8.2. Surface plots for the C^{-1} - $P_2(T)/P_2(\partial T)/P_1(\partial T)/P_0(T)$ element on the unit square domain Ω_1 ; left for the primal variable u_h ; right for the dual variable λ_0 .

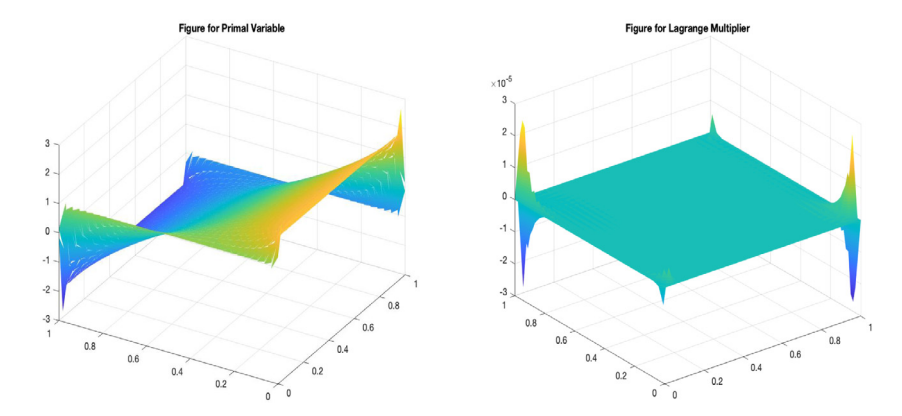


Fig. 8.3. Surface plots for the C^0 - $P_2(T)/P_1(\partial T)/P_1(T)$ element on the unit square domain Ω_1 ; left for the primal variable u_h ; right for the dual variable λ_0 .

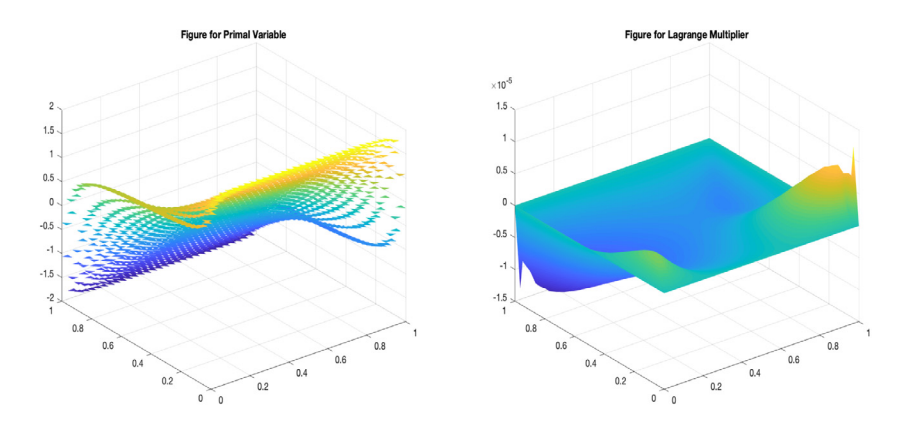


Fig. 8.4. Surface plots for the C^0 - $P_2(T)/P_1(\partial T)/P_0(T)$ element on the unit square domain Ω_1 ; left for the primal variable u_h ; right for the dual variable λ_0 .

element is used and the one on the right is for the numerical solution u_h with the C^0 -type $P_2(T)/P_1(\partial T)/P_0(T)$ element. Note that the exact solution for the primal variable in the configuration is u = x. We conclude that the numerical solution u_h obtained by PDWG scheme is consistent with the exact solution.

Fig. 8.6 shows the plots for the numerical solution u_h on the unit square domain Ω_1 when the C^0 -type $P_2(T)/P_1(\partial T)/P_0(T)$ element is employed to the test problem with convective direction $\mathbf{b} = [1,0]$ and load function f = 1. The Neumann boundary condition of $g_2 = a_{11}$ (where $a = (a_{ij})$) is imposed on the inflow boundary edge $\{0\} \times (0,1)$ and the Dirichlet boundary condition $g_1 = 0$ is imposed on the rest of the boundary. Fig. 8.6 shows the numerical solution u_h for different

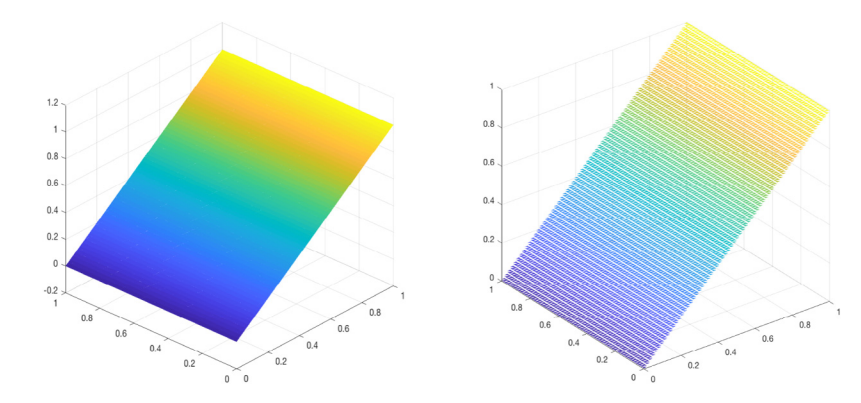


Fig. 8.5. Surface plot of u_h on the unit square domain Ω_1 : left for the C^0 - $P_2(T)/P_1(\partial T)/P_1(T)$ element, right for the C^0 - $P_2(T)/P_1(\partial T)/P_0(T)$ element.

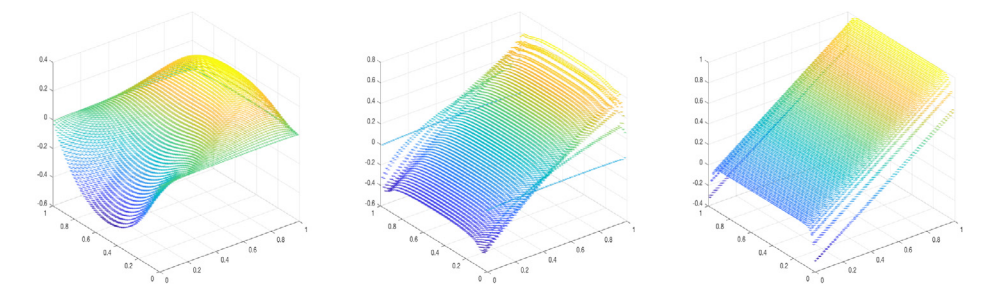


Fig. 8.6. Surface plots for the primal variable u_h on the unit square domain Ω_1 with the C^0 - $P_2(T)/P_1(\partial T)/P_0(T)$ element: left for the diffusion tensor $a = [10^{-1}, 0; 0, 10^{-1}]$, middle for the diffusion tensor $a = [10^{-3}, 0; 0, 10^{-3}]$, right for the diffusion tensor $a = [10^{-6}, 0; 0, 10^{-6}]$.

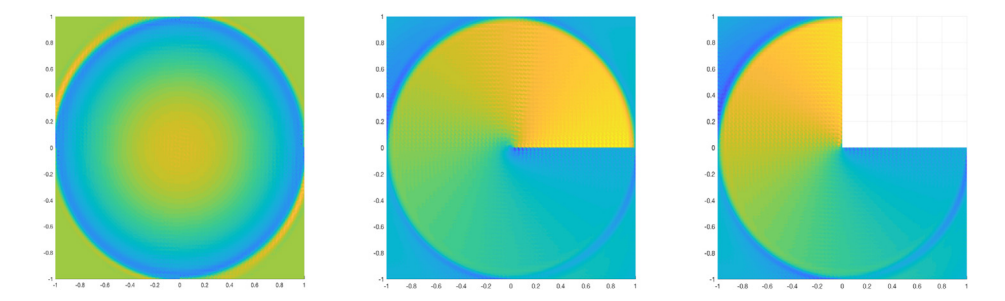


Fig. 8.7. Contour plots for the primal variable u_h : left for the square domain Ω_3 ; middle for the cracked square domain Ω_4 ; and right for the L-shaped domain Ω_5 .

diffusion tensors: $a = [10^{-1}, 0; 0, 10^{-1}]$ (left), $a = [10^{-3}, 0; 0, 10^{-3}]$ (middle), and $a = [10^{-6}, 0; 0, 10^{-6}]$ (right). The exact solutions for the primal variable in the configurations are unknown. However, we can see from Fig. 8.6 that when the diffusion tensor becomes smaller, the boundary layer phenomena is more clear.

Fig. 8.7 illustrates the contour plots for the numerical solution u_h arising from the primal-dual weak Galerkin finite element method on three different domains: (i) the square domain $\Omega_3 = (-1, 1)^2$, (ii) the cracked square domain Ω_4 , and (iii) the L-shaped domain Ω_5 . In this numerical experiment, the model problem has a diffusion tensor $a = [10^{-4}, 0; 0, 10^{-4}]$ and a convective (rotational) vector $\mathbf{b} = [y, -x]$. Fig. 8.7 is obtained by using the following configurations: (a) the $C^0 - P_2(T)/P_1(\partial T)/P_1(T)$ element, (b) Neumann boundary condition $g_2 = 0$ on the inflow boundary edges ($\mathbf{b} \cdot \mathbf{n} < 0$), (c) Dirichlet boundary condition $g_1 = \sin(3x)$ on the outflow boundary edges ($\mathbf{b} \cdot \mathbf{n} > 0$); and (d) the load function f = 1. Note that no exact solutions for the primal variable are known in the configurations. However, some interesting and trustable numerical solutions arising from PDWG method are illustrated in Fig. 8.7.

In summary, the numerical performance of the PDWG schemes (4.4)–(4.5) for the convection-dominated convection-diffusion problem (1.1) is typically consistent with or better than what our theory predicts. Theorem 7.1 and the numerical tests show that the stabilization parameter γ is not necessary to make the PDWG method convergent and accurate when s = k - 1. We conjecture that the PDWG finite element scheme with $\gamma = 0$ is stable and has the optimal order of convergence for both s = k - 2 and s = k - 1 when the diffusion tensor a and the convection vector b are uniformly

piecewise continuous functions, provided that the meshsize is sufficiently small. Interested readers are encouraged to explore the corresponding theory with more sophisticated mathematical tools.

9. Conclusions

The primal-dual weak Galerkin finite element method developed here for convection-diffusion problems has shown several promising features as a discretization approach in the following aspects: (1) it provides a symmetric and well-posed discrete problem; (2) it is consistent in the sense that the exact solution, if sufficiently regular, satisfies the discrete variational problem; (3) it allows for low regularity of the primal variable and admits optimal a priori error estimates. Further exploration is needed for constructing fast solvers for the resulting discrete problems and this is a subject of a current and future work.

Acknowledgments

The authors would like to thank Dr. Junping Wang for his valuable discussion and suggestions, and Dan Li (Northwestern Polytechnical University, China) for sharing the C^{-1} WG-element code developed jointly with one of the authors. The authors also thank the anonymous referees for raising several important points and providing key suggestions for improving the manuscript.

References

- [1] H.C. Elman, A. Ramage, An analysis of smoothing effects of upwinding strategies for the convection-diffusion equation, SIAM J. Numer. Anal. 40 (2002) 254–281, http://dx.doi.org/10.1137/S0036142901374877.
- [2] H.G. Roos, M. Stynes, L. Tobiska, Robust Numerical Methods for Singularly Perturbed Differential Equations. Convection-Diffusion-Reaction and Flow Problems, second ed., in: Springer Ser. Comput. Math., vol. 24, Springer, Berlin, 2008.
- [3] J.J.H. Miller, E.O'. Riordan, G.I. Shishkin, Fitted Numerical Methods for Singular Perturbation Problems, Error Estimates in the Maximum Norm for Linear Problems in One and Two Dimensions, World Scientific, River Edge, NJ, 1996.
- [4] J. Xu, L. Zikatanov, A monotone finite element scheme for convection-diffusion equations, Math. Comp. 68 (228) (1999) 1429-1446.
- [5] R. Lazarov, L. Zikatanov, An exponential fitting scheme for general convection-diffusion equations on tetrahedral meshes, J. Comput. Appl. Math. 1 (92) (2005) 60–69.
- [6] T.J.R. Hughes, A. Brooks, A multidimensional upwind scheme with no crosswind diffusion, in: T.J.R. Hughes (Ed.), Finite Element Methods for Convection Dominated Flows, in: AMD 34, Amer. Soc. Mech. Engrs. (ASME), New York, 1979, pp. 19–35.
- [7] A.N. Brooks, T.J.R. Hughes, Streamline upwind/Petrov–Galerkin formulations for convection dominated flows with particular emphasis on the incompressible Navier–Stokes equations, Comput. Methods Appl. Mech. Engrg. 32 (1982) 199–259.
- [8] N.S. Bakhvalov, On the optimization of the methods for solving boundary value problems in the presence of a boundary layer, Mat. Mat. Fiz. 9 (1969) 841–859, (in Russian).
- [9] G.I. Shishkin, Grid Approximation of Singularly Perturbed Elliptic and Parabolic Equations (Second doctoral thesis), Keldysh Institute, Moscow, 1990. (in Russian).
- [10] I. Babuška, The selfadaptive approach in the finite element method, in: The Mathematics of Finite Elements and Applications II, in: Proceedings of the Second Brunel University Conference at the Institute of Mathematics and Applications, Uxbridge, 1975, Academic Press, London, 1976, pp. 125–142.
- [11] C. De Boor, Good approximation by splines with variable knots, in: Spline Functions and Approximation Theory, in: Proceedings of the Symposium, Edmonton, 1972, pp. 57–72.
- [12] H.J. Reinhardt, A posteriori error estimates and adaptive finite element computations for singularly perturbed one space dimensional parabolic equations, in: Analytical and Numerical Approaches to Asymptotic Problems in Analysis, in: Proceedings of the Conference, Nijmegen, The Netherlands, 1980, North-Holland Math. Stud., vol. 47, North-Holland, Amsterdam, 1981, pp. 213–233.
- [13] I. Babuška, The finite element method with penalty, Math. Comp. 27 (1973) 221-228.
- [14] J. Douglas Jr., T. Dupont, Interior penalty procedures for elliptic and parabolic Galerkin methods, in: Second International Symposium on Computing Methods in Applied Sciences, Versailles, 1975, in: Lecture Notes in Phys., vol. 58, Springer, Berlin, 1976, pp. 207–216.
- [15] W.H. Reed, T.R. Hill, Triangular Mesh Methods for the Neutron Transport Equation, Technical report LA-UR-73-0479, Los Alamos Scientific Laboratory, Los Alamos, NM, 1973.
- [16] M.F. Wheeler, An elliptic collocation-finite element method with interior penalties, SIAM J. Numer. Anal. 15 (1978) 152-161.
- [17] D.N. Arnold, F. Brezzi, B. Cockburn, L.D. Marini, Unified analysis of discontinuous Galerkin methods for elliptic problems, SIAM J. Numer. Anal. 39 (2002) 1749–1779.
- [18] C. Johnson, Numerical Solution of Partial Differential Equations by the Finite Element Method, Cambridge University Press, Cambridge, 1987.
- [19] B. Ayuso, L.D. Marini, Discontinuous Galerkin methods for advection-diffusion-reaction problems, SIAM J. Numer. Anal. 47 (2009) 1391–1420.
- [20] C.E. Baumann, J.T. Oden, A discontinuous hp finite element method for convection diffusion problems, Comput. Methods Appl. Mech. Engrg. 175 (1999) 311–341.
- [21] A. Buffa, T.J.R. Hughes, G. Sangalli, Analysis of a multiscale discontinuous Galerkin method for convection-diffusion problems, SIAM J. Numer. Anal. 44 (2006) 1420–1440.
- [22] J. Guzman, Local analysis of discontinuous Galerkin methods applied to singularly perturbed problems, J. Numer. Math. 14 (2006) 41–56.
- [23] P. Houston, C. Schwab, E. Suli, Discontinuous hp-finite element methods for advection diffusion-reaction problems, SIAM J. Numer. Anal. 39 (2002) 2133–2163.
- [24] T.J.R. Hughes, G. Scovazzi, P.B. Bochev, A. Buffa, A multiscale discontinuous Galerkin method with the computational structure of a continuous Galerkin method, Comput. Methods Appl. Mech. Engrg. 195 (2006) 2761–2787.
- [25] J.S. Hesthaven, T. Warburton, Nodal Discontinuous Galerkin Methods: Algorithms, Analysis, and Applications, in: Texts Appl. Math., vol. 54, Springer, New York, 2008.
- [26] E. Burman and, C. He, Primal dual mixed finite element methods for indefinite advection-diffusion equations, arXiv:1811.00825.
- [27] E. Burman, M. Nechita, L. Oksanen, A stabilized finite element method for inverse problems subject to the convection–diffusion equation. I: diffusion-dominated regime, arXiv:1811.00431.

- [28] C. Wang, A new primal-dual weak galerkin finite element method for ill-posed elliptic cauchy problems, Journal of Computational and Applied Mathematics 371 (2020) 112629.
- [29] C. Wang, J. Wang, Primal-dual weak Galerkin finite element methods for elliptic Cauchy problems, Comput. Math. Appl. 79 (3) (2020) 746-763.
- [30] C. Wang, J. Wang, A primal-dual weak Galerkin finite element method for second order elliptic equations in non-divergence form, Math. Comput., Math. Comp. 87 (2018) 515–545.
- [31] C. Wang, J. Wang, A primal-dual weak Galerkin finite element method for Fokker-Planck type equations, SIAM J. Numer. Anal. 58 (5) (2020) 2632–2661, arXiv:1704.05606, in press.
- [32] E. Burman, Stabilized finite element methods for nonsymmetric, noncoercive, and ill-posed problems. Part I: Elliptic equations, SIAM J. Sci. Comput. 35 (6) (2013) A2752–A2780.
- [33] E. Burman, Stabilized finite element methods for nonsymmetric, noncoercive, and ill-posed problems. Part II: Hyperbolic equations, SIAM J. Sci. Comput. 36 (4) (2014) A1911–A1936.
- [34] E. Burman, Error estimates for stabilized finite element methods applied to ill-posed problems, C. R. Math. Acad. Sci. Paris 352 (7-8) (2014) 655-659.
- [35] E. Burman, Stabilised finite element methods for ill-posed problems with conditional stability, in: Building Bridges: Connections and Challenges in Modern Approaches to Numerical Partial Differential Equations, 93–127, in: Lect. Notes Comput. Sci. Eng., vol. 114, Springer, 2016.
- [36] E. Burman, A stabilized nonconforming finite element method for the elliptic Cauchy problem, Math. Comp. 86 (303) (2017) 75-96.
- [37] E. Burman, P. Hansbo, Stabilized nonconforming finite element methods for data assimilation in incompressible flows, Math. Comp. 87 (311) (2018) 1029–1050.
- [38] E. Burman, M.G. Larson, L. Oksanen, Primal-dual mixed finite element methods for the elliptic Cauchy problem, SIAM J. Numer. Anal. 56 (6) (2018) 3480-3509.
- [39] D. Adak, E. Natarajan, A unified analysis of nonconforming virtual element methods for convection diffusion reaction problem, arXiv: 1601.01077v1.
- [40] S. Berrone, A. Borio, G. Manzini, SUPG stabilization for the nonconforming virtual element method for advection-diffusion-reaction equations, arXiv:1806.00879v1.
- [41] D. Irisarri, Virtual element method stabilization for convection–diffusion-reaction problems using the link-cutting condition, Calcolo 54 (2017) 141–154.
- [42] G. Chen, W. Hu, J. Shen, J. Singler, Y. Zhang, X. Zheng, An HDG method for distributed control of convection diffusion PDEs, J. Comput. Appl. Math. 343 (2018) 643–661.
- [43] Y. Chen, Analysis of variable-degree HDG methods for convection-diffusion equations, Part I: general nonconforming meshes, IMA J. Numer. Anal. 32 (2012) 1267–1293.
- [44] W. Gong, W. Hu, M. Mateos, J. Singler, X. Zhang, Y. Zhang, A new HDG method for Dirichlet boundary control of convection diffusion PDEs II: Low regularity, SIAM J. Numer. Anal. 56 (4) (2018) 2262–2287.
- [45] W. Hu, J. Shen, J. Singler, Y. Zhang, X. Zheng, An HDG method for distributed control of convection diffusion PDEs, arXiv:1801.00082v1.
- [46] B. Cockburn, B. Dong, J. Guzman, M. Restelli, R. Sacco, A hybridizable discontinuous Galerkin method for steady-state convection-diffusion-reaction problems, SIAM J. Sci. Comput. 31 (5) (2009) 3827–3846.
- [47] B. Cockburn, The weak Galerkin methods are rewritings of the hybridizable discontinuous Galerkin methods, arXiv:1812.08146.
- [48] L. Chen, Equivalence of weak Galerkin methods and virtual element methods for elliptic equations, arXiv:1503.04700.
- [49] Q. Hong, J. Xu, Uniform stability and error analysis for some discontinuous Galerkin methods, arXiv:1805.09670.
- [50] Jan Chabrowski, The Dirichlet Problem with L²-Boundary Data for Elliptic Linear Equations, in: Lecture Notes in Mathematics, vol. 1482, Springer-Verlag, Berlin, 1991.
- [51] Martin Costabel, Boundary integral operators on Lipschitz domains: elementary results, SIAM J. Math. Anal. 19 (3) (1988) 613-626.
- [52] Norbert Wiener, Discontinuous boundary conditions and the Dirichlet problem, Trans. Amer. Math. Soc. 25 (3) (1923) 307-314.
- [53] Norbert Wiener, Trans. Amer. Math. Soc. 26 (4) (1924) 494, Errata; Discontinuous boundary conditions and the dirichlet problem, Trans. Amer. Math. Soc. 25 (3) (1923) 307–314, 1501246.
- [54] V. Girault, P. Raviart, Finite Element Methods for Navier-Stokes Equations, Theory and Algorithms, Springer-Verlag, Berlin Heidelberg, New York, Tokyo, 1979.
- [55] J. Wang, X. Ye, A weak Galerkin mixed finite element method for second-order elliptic problems, Math. Comp. 83 (2014) 2101-2126.